

Chapter 4

Controlling Polyamide Dimerization through Non-Covalent Interactions

Abstract

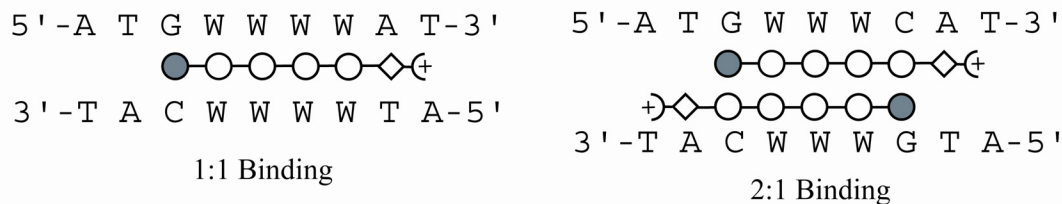
Due to size limitations on the cellular uptake of polyamides, we herein investigate whether side-by-side dimerization of polyamides can be accomplished through non-covalent interactions. A series of novel pyrrole rings were synthesized and incorporated into 5-ring polyamides. We find that functionalization of the N1 position of pyrrole with positively interacting side chains is unable to control polyamide dimerization. Functionalization with negatively interacting side chains is able to control hetero- and homodimerization.

Introduction

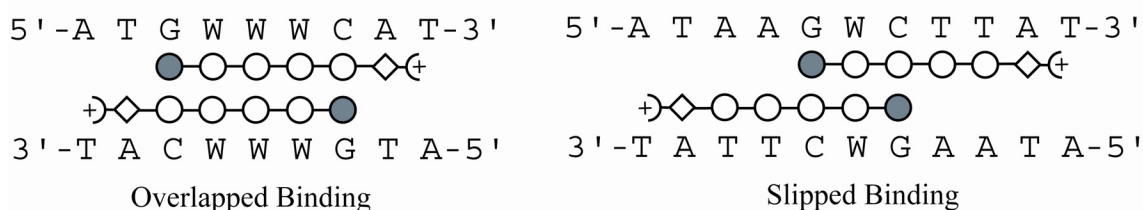
While increasing the number of pyrrole and imidazole rings in a given polyamide increases binding affinity, cellular uptake studies have shown that polyamides containing more than eight rings are unable to reach their target DNA within the nuclei of live cells. The goal of the research reported herein is to design polyamide systems capable of targeting large (6–10 bp) sequences of DNA with high affinity and specificity, while at the same time possessing favorable cellular and nuclear uptake properties.

Nature uses a variety of non-covalent forces to create specific protein folds and to associate multiple proteins into complexes.¹ A notable example is the ribosomal complex, which consists of over 30 proteins and ribonucleic (RNA) fragments held together by non-covalent interactions.² These forces include van der Waals forces, hydrogen bonding, Coulombic forces, and cation- π interactions.^{1, 3-6} Non-covalent forces are likewise responsible for the binding of polyamide molecules to DNA. While linking the two strands of the 2:1 polyamide/DNA complex covalently greatly increases the binding affinity, the size of the polyamide is doubled and cellular uptake may be compromised. Perhaps unlinked polyamide strands can be functionalized in such a way that imparts some non-covalent associative force between the two strands, leading to increased affinity and specificity. However, because the forces are non-covalent, and the polyamide strands are not associated until bound to DNA, the smaller polyamide strands may possess favorable uptake properties. Thus, with this system, both the goal of cellular uptake and that of specific and high affinity recognition of DNA may be realized.

2:1 vs 1:1 Polyamide: DNA Stoichiometry



Fully Overlapped vs. Slipped



Distinct Fully Overlapped Sites

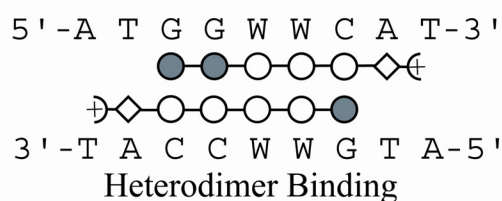
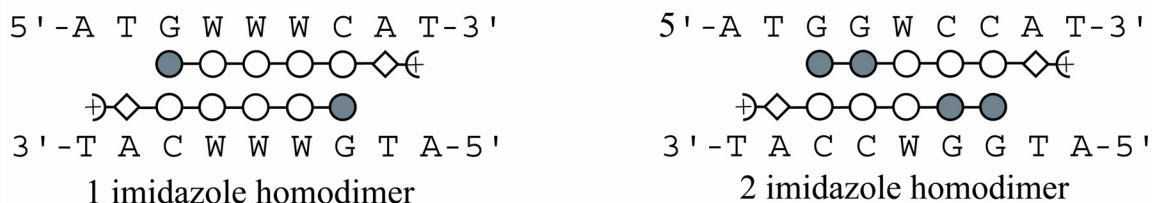


Figure 4.1. Schematic model for illustrating the various binding modes possible when DNA is incubated with two different polyamides. Imidazole and pyrrole are represented by dark and light circles, respectively.

Dimeric DNA/polyamide complexes are inherently ambiguous. As shown schematically in Figure 4.1, when DNA is incubated with two different polyamide strands, multiple binding sites can be targeted. New functional groups incorporated onto unlinked dimers must be able to select for one or a few of the myriad binding modes while at the same time not interfering with the polyamide's DNA recognition elements.

The problem of heterodimer versus homodimer formation within the fully overlapped, 2:1 binding motif is the subject of this research report.

Polyamide Functionalization.

When polyamides bind to DNA the N1-methyl position of each pyrrole and imidazole subunit points up from the floor of the minor groove into solvent. Additionally, paired pyrrole and imidazole residues place their N-methyl groups in close proximity.⁷ Functionalization of polyamides at this position would be ideal because groups placed here would be able to interact based on their close proximity, and would not interfere with the DNA-recognition side of the polyamide (Figure 4.2).

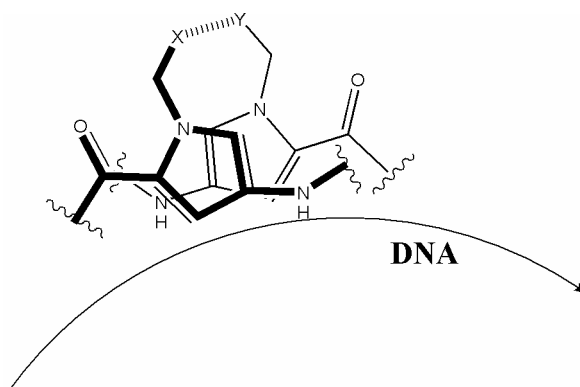


Figure 4.2. Structure of two polyamide strands bound dimerically in the minor groove of DNA. Functionalization of the polyamides with “X” and “Y” at the N1 position of pyrrole will place new moieties in close proximity without interfering with the DNA-recognition face of the polyamide.

The polyamide ImPyPyPyPy- β -Dp (**PA1**) had previously been analyzed by DNase I footprinting and was shown to bind with submicromolar affinity.⁸ In this study, **PA1** is tested along with the polyamide ImImPyPyPy- β -Dp (**PA2**). The designed plasmid incorporates binding sites for both **PA1** and **PA2** homodimers as well as the site for the

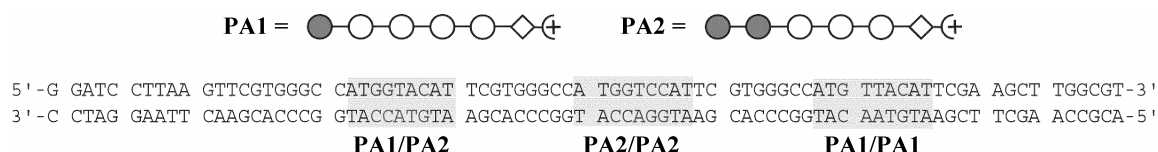


Figure 4.3. Sequence of plasmid insert pDHN2 used to probe homodimer vs. heterodimer formation. The plasmid contains binding sites for each of the two homodimers (center, right) and for the heterodimer (left).

PA1/PA2 heterodimer (Figure 4.3). This plasmid is designed to probe whether polyamide N1 functionalization will be able to control the relative affinities of polyamide dimers for the three distinct sites. This system allows for the central Py/Py pair to be functionalized as in Figure 4.2, and non-covalent interactions probed. Figure 4.4 shows schematically the functional groups probed in this study. Several biologically relevant interactions such as sterics, hydrogen bonding, quadrupole interaction, and cation- π are represented in this series. New pyrrole rings functionalized as shown below were synthesized, incorporated into polyamides, and their ability to drive specific dimer formation probed by quantitative DNase I footprinting.⁹

Synthesis of New Monomers (Figure 4.5).

A novel isobutyl imidazole trichloroketone was used as a replacement for the 1-methyl imidazole cap, was made in 84% yield from compound 2-trichloroketo imidazole, which was prepared according to published procedures.¹⁰

Monomer **7i** was prepared by Nick Wurtz. All other Boc-protected, N1-functionalized pyrrole amino acids were synthesized as shown in Figure 4.5. N1 alkylation was achieved from the 4-nitro or 4-NHBoc 2-ester pyrroles (**1**, **2**, **3**, **4**) using various alkyl bromides of the form Br-R (R = **a-f**, **h**, **k**), tetrabutylammonium iodide, and potassium carbonate in acetone with yields ranging from 70–99%. For the base-labile phthalimide-

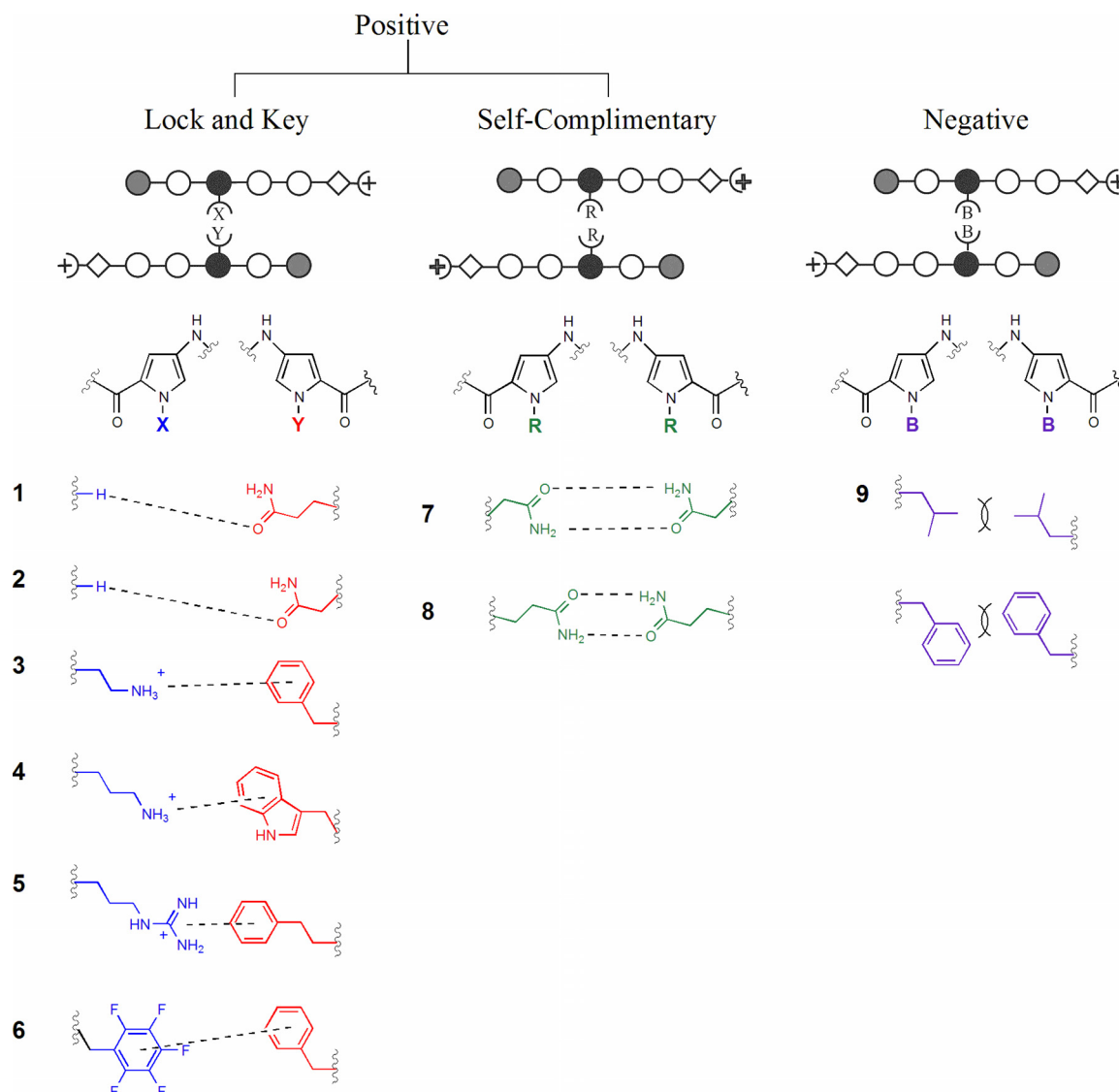


Figure 4.4. Schematic and structural representation of the non-covalent interactions reported herein. **Lock-and-Key** (left): Two different functional groups provide a stabilizing interaction. Examples include hydrogen bonding (1, 2), Cation- π (3-5), and quadrupole interactions (6). **Positive Interaction** (center): Two identical side chains interact to provide a stabilizing force. Examples include hydrogen bonding (7, 8) between two primary amides. **Negative Interaction** (right): Two identical side chains interact negatively to destabilize the pairing. Examples include steric exclusion from bulky groups (9, 10). Associative forces are represented by dashed lines; steric clash is represented by overlapping arcs.

protected amines (**a** and **e**), the pyrrole trimethylsilyl ethyl (TMSE) ester¹¹ was used in order to effect ester hydrolysis using tetrabutylammonium fluoride without disturbing the phthalimide moiety. The TMSE ester was also used when making pentafluorobenzyl derivative **b** in order to avoid degradation of the product during the basic hydrolysis of

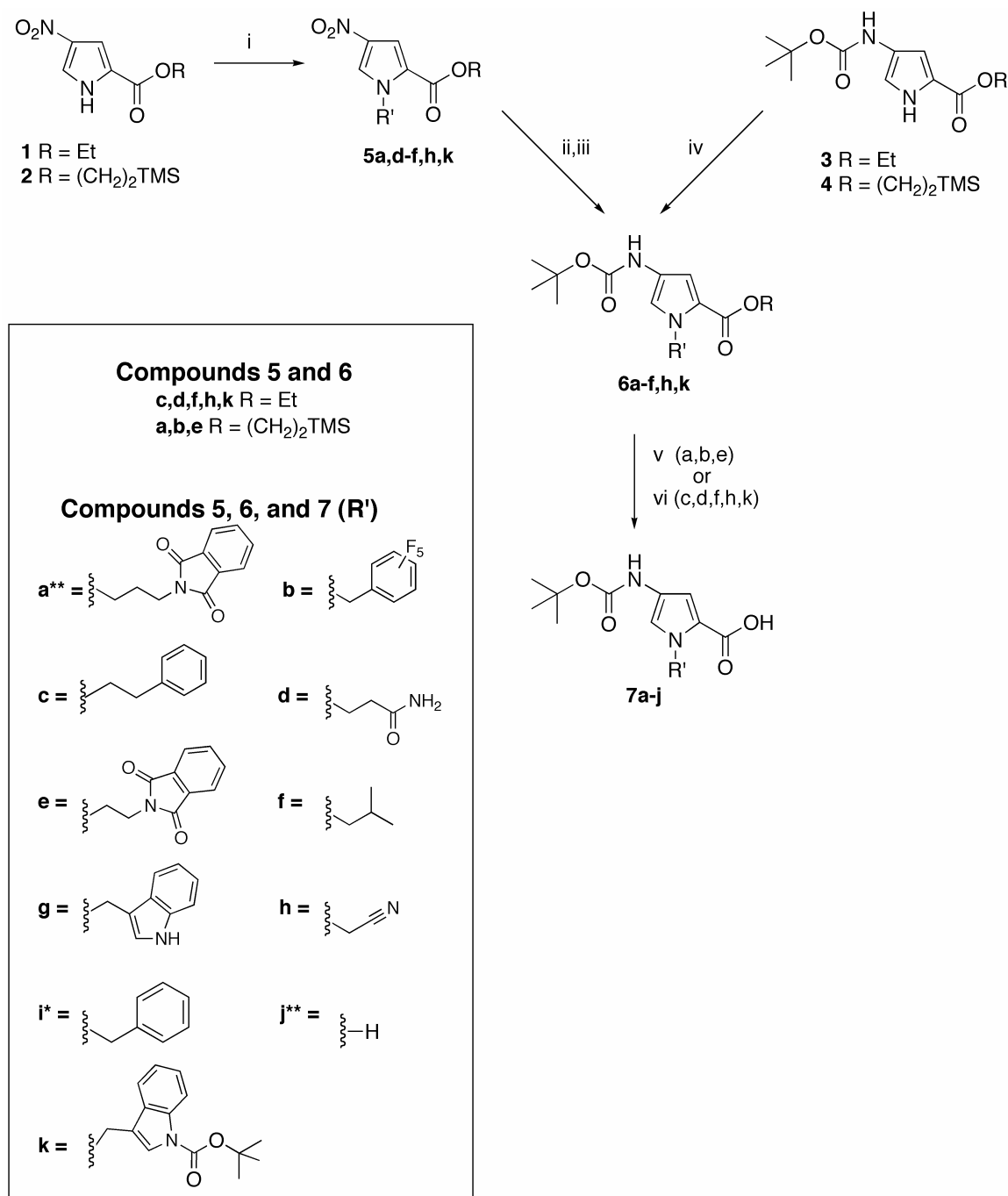


Figure 4.5. Synthetic scheme for novel N-functionalized pyrrole monomers. i) Br-R(**a**, **d–h**), K₂CO₃, Bu₄NI, acetone; ii) 10% Pd/C, H₂, EtOAc; iii) Boc₂O, 1M NaHCO₃; iv) Br-R (**b**, **c**), K₂CO₃, Bu₄NI, acetone; v) TBAF, THF; vi) 2M NaOH, EtOH. (*) Compound provided by Nick Wurtz. (**) Compound prepared as previously published.

the ethyl ester precursor. Alkylations with both the pentafluorobenzyl and ethylbenzyl bromides were performed on the more advanced 4-NHBoc 2-TMSE ester pyrrole (**4**)

because of the greater reactivity of the bromides. All other N1- modifications were carried out via alkylation of the nitro ethyl ester pyrrole **1**.¹² Subsequent reduction using palladium on carbon under an atmosphere of hydrogen gas, followed by Boc- protection using Boc anhydride, afforded **6a, d, e, f, and g** in high yields. The Boc-protected carboxylic acid final products **7a–j** were obtained in high yields from either the ethyl- or TMSE- protected intermediates **6a–f, h, k**. Treatment of **6k** with base hydrolyzed the ester and deprotected the Boc-indole in one step, affording **7g** in 97% yield.

Synthesis of Polyamides.

Unfunctionalized Polyamides (**PA1** and **PA2**) were synthesized from pyrrole and imidazole Boc-protected amino acids on solid support.¹³ Polyamides **PA3–PA5, PA8–PA15, and PA17–PA24** (Figure 4.6) were synthesized on solid support using monomers **7a–j** and **9** along with the standard imidazole and pyrrole monomers (Figure 4.7). Coupling of the isobutyl trichloro ketone cap (**9**) was carried out using 1.0 equivalent of resin-bound amine, 2.0 equivalents of **9**, and 1.0 equivalents of diisopropylethylamine (DIEA) in DMF at 37 °C for two hours in high conversion as determined by reversed-phase HPLC. Polyamide ImPyPy(3G)PyPy-β-Dp (Propylguanidyl side chain: **PA16**) was synthesized in 5% isolated yield from resin-bound ImPyPy(3P)PyPy-β-RESIN (Propylamino side chain) and N,N'-Boc-guanidyl pyrazole followed by deprotection. Initial attempts to synthesize polyamides ImPy(Am)PyPyPy-β-Dp (amide side chain: **PA6**) and ImImPyPy(Am)Py-β-Dp (amide side chain: **PA7**) were carried out using a Boc-protected pyrrole carboxylic acid functionalized on N1 with the primary amide

group ($-\text{CH}_2\text{CONH}_2$). However, activation of this monomer using standard activating agents (DCC/HOBt, HBTU, Py-BOP) led to the intramolecular attack of the amide

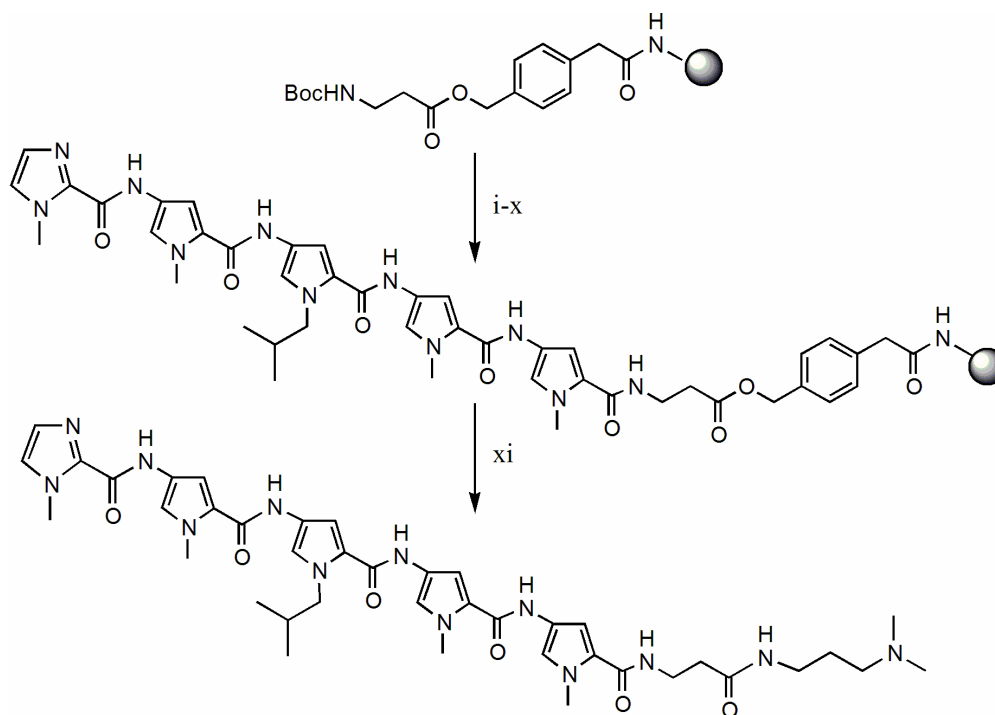


Figure 4.6. Representative solid-phase synthetic scheme for ImPyPy(iBu)PyPy- β -Dp (**PA3**) from Boc- β -Ala-PAM resin. i) 50% TFA:DCM; ii) Boc-Py-OBt, DIEA, NMP; iii) 50% TFA:DCM; iv) Boc-Py-OBt, DIEA, NMP; v) 50% TFA:DCM; vi) Boc-Py(iBu)-OH, HBTU, DIEA, NMP; vii) 50% TFA:DCM; viii) Boc-Py-OBt, DIEA, NMP; ix) 50% TFA:DCM; x) Im-OH, HBTU, DIEA, NMP; xi) Dimethylamino propyl amine, 55 °C, 12 h.

functionality on the activated ester, forming an unreactive bicyclic by-product. To overcome this difficulty, an attempt was made to form **PA6** and **PA7** by alkylating ImDsPyPyPy- β -Dp (**PA10**) and ImImPyDsPy- β -Dp (**PA11**) (Ds = Des-methyl pyrrole monomer¹²) with potassium carbonate and bromoacetamide. ^1H NMR analysis of the alkylated product showed that the tail dimethylammonium nitrogen was the site of alkylation. Subsequent analysis shows that potassium carbonate is not basic enough to deprotonate the pyrrole ring (pK_a of pyrrole in DMSO = 23), thus making the dimethylalkylammonium nitrogen the most reactive nucleophile.

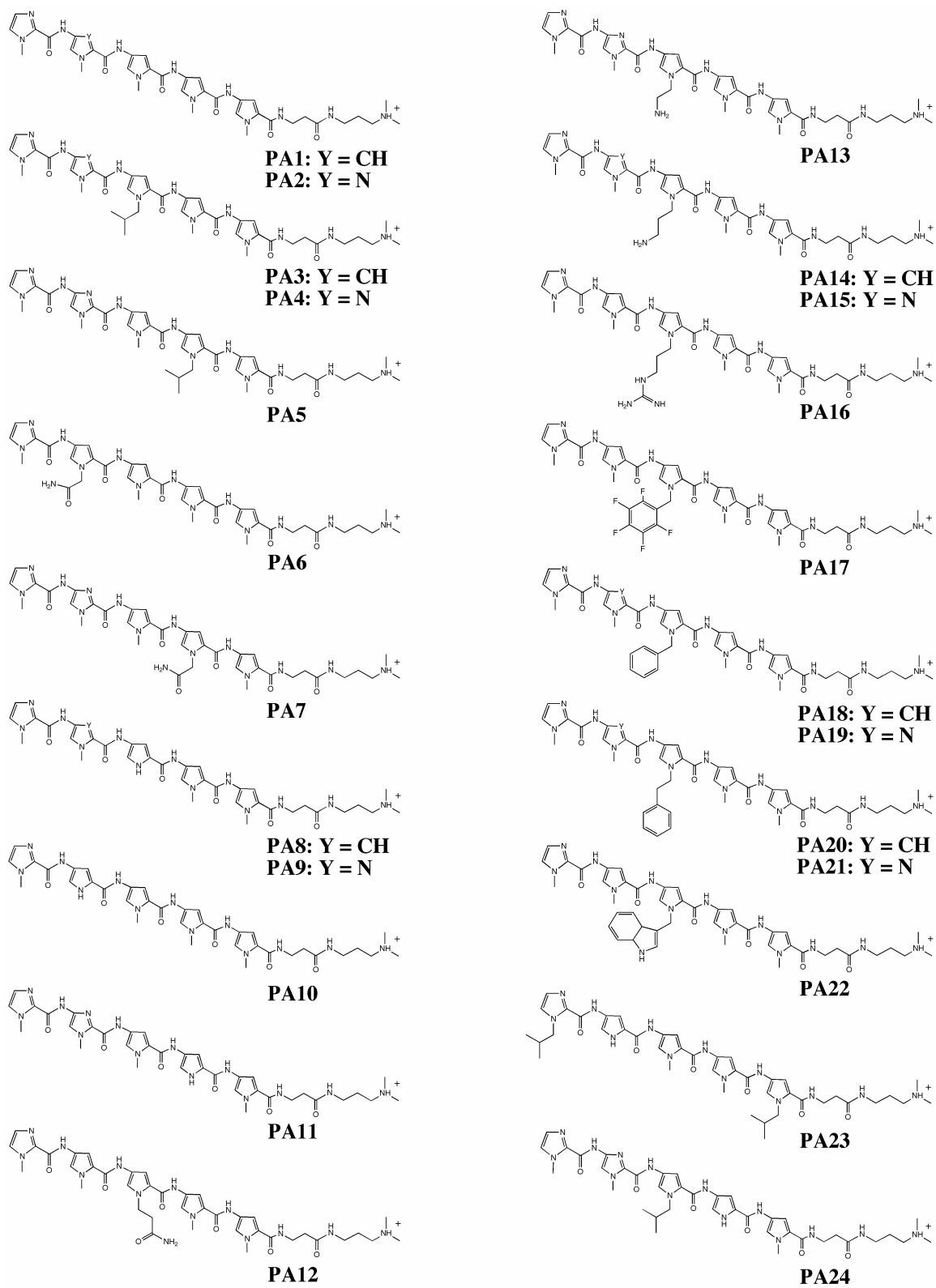


Figure 4.7. Chemical structures of the 5-ring polyamides synthesized on solid support.

By pre-incubating **PA10** and **PA11** with 10.0 equivalents of sodium hydride in DMF, a global deprotonation was achieved. Upon addition of one equivalent of bromoacetamide, the monoalkylated products **PA6** and **PA7** were obtained in 30% yield. Alternatively, monomer **7h** could be used in the standard solid-phase protocol. Upon acidic workup, the nitrile is hydrated to give **PA6** and **PA7** in 5% isolated yield. While the yields of the two methods seem very different, the 5% yield is the amount of isolated product after two steps, cleavage from resin and HPLC purification. The seemingly higher 30% yield represents the amount of product isolated after a single HPLC purification only. With respect to overall yield, the two methods do not differ significantly. The purity and identity of each polyamide was determined by reversed-phase HPLC, MALDI-TOF mass spectrometry, and ^1H NMR.

Quantitative DNase I Footprinting.

Equilibrium association constants (K_a) were determined using DNase I footprint titration experiments (10 mM Tris HCl, 10 mM KCl, 10 mM MgCl_2 , and 5 mM CaCl_2 , pH 7.0, 22 °C). Plasmid pDHN2¹⁴ contains three match sites: 5'-TGTTACA-3' is a match site for the one-imidazole homodimer (**PA1/PA1**), 5'-TGGTCCA-3' is a match site for the two-imidazole homodimer (**PA2/PA2**), and 5'-TGGTACA-3' is a match site for the heterodimer formed between the one- and two-imidazole compounds (**PA1/PA2**). The parent polyamides were footprinted against pDHN2 and their binding affinities determined for reference. **PA1** binds as a homodimer to its match site with an affinity of $5.2 \times 10^8 \text{ M}^{-1}$. **PA2** binds to its homodimer match site with an affinity of $4.8 \times 10^8 \text{ M}^{-1}$. The **PA1/PA2** heterodimer binds its match site with a similar affinity of $4.2 \times 10^8 \text{ M}^{-1}$.

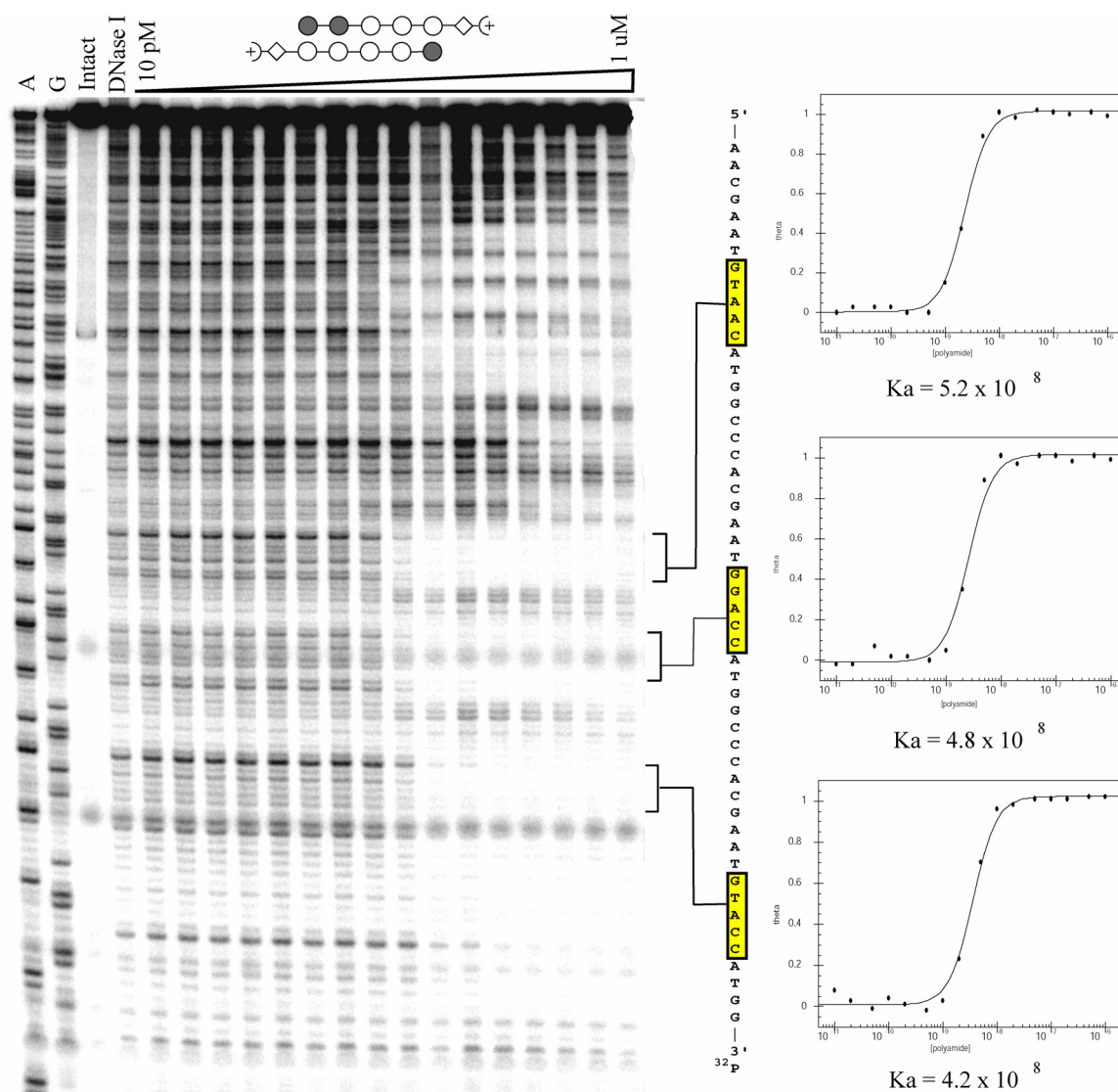


Figure 4.8. Quantitative DNase footprinting experiment with ImPyPyPy- β -Dp (**PA1**) and ImImPyPyPy- β -Dp (**PA2**) on the 3'- 32 P-labeled restriction fragment pDHN2. Gel lanes from left to right: A reaction, G reaction, intact DNA, DNase I standard, DNase digestion products in the presence of 10 pM, 20 pM, 50 pM, 100 pM, 200 pM, 500 pM, 1 nM, 2 nM, 5 nM, 10 nM, 20 nM, 50 nM, 100 nM, 200 nM, 500 nM, 1 μ M polyamide. Right: Quantitation and Hill plots of data from gel. Below each plot is the binding affinity constant obtained at each site (K_a in M^{-1}). Conditions and data analysis as outlined in the text.

(Figure 4.8). Association constants for functionalized polyamides are compared to these parent values to determine the functional group's ability to select for one of the three binding modes. As an initial screen for binding, compounds were tested on the one-imidazole homodimer match site with the side chains of interest paired across from each

other on the central pyrrole residue. Compounds that were either ambiguous or promising in this system were tested on the heterodimer site. Each equilibrium association constant is an average of at least three quantitative DNase I footprint titrations. The footprinting results are summarized in Table 4.1. With respect to the parent, unfunctionalized polyamides (**PA1** and **PA2**), several interesting features emerge from these data. Firstly, both ImPyPy(Bz)PyPy- β -Dp (benzyl side chain: **PA18**) and ImPyPy(iBu)PyPy- β -Dp (isobutyl side chain: **PA3**) exhibit a 16-fold reduction in binding affinity when homodimerically paired within the minor groove. Interestingly, ImPyPy(5FBz)PyPy- β -Dp (pentafluorobenzyl moiety: **PA17**), which is isosteric to the benzyl group while carrying the opposite quadrupole, does not alter binding affinity relative to the parent compound.

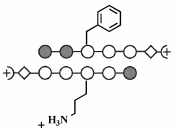
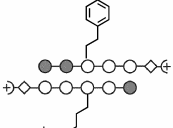
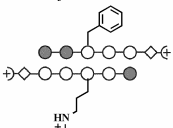
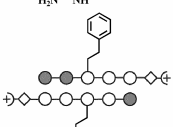
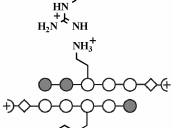
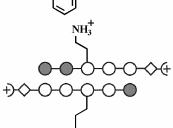
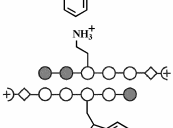
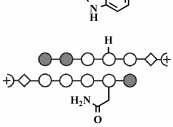
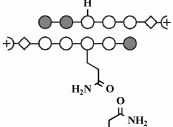
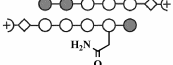
Alternatively, each of the positively charged side chains exhibits an increased affinity when homodimerically paired. Both ImPyPy(3G)PyPy- β -Dp (propylguanidyl side chain: **PA16**) and ImPyPy(3P)PyPy- β -Dp (propylamino side chain: **PA14**) bind to their match sites with a K_a of $6.6 \times 10^9 \text{ M}^{-1}$. This affinity represents a greater than 10-fold increase over the parent polyamides. ImImPy(2P)PyPy- β -Dp (ethylamino side chain: **PA13**) gives only a 3-fold binding affinity increase. Likewise, the hydrogen side chain of ImPyDsPyPy- β -Dp (**PA8**) exhibits a 4-fold increase in affinity.

When examining heterodimeric side chain pairings, each of the proposed cation/ π interactions between the positively-charged side chains (**PA13–PA16**) paired with the three aromatic side chains (**PA18–PA22**) exhibit affinities within a factor of 3 from the parent polyamides. The propylamino moiety of **PA15**, paired with either the benzyl (**PA18**) or ethylbenzyl (**PA20**) side chains shows a slight increase in affinity while the

Table 2: Equilibrium Association Constants*

PA #	Polyamide	5'-TGGTACA-3'	5'-TGGTCCA-3'	5'-TGTTACA-3'	$\Delta K_{a(\text{parent})}$
1 + 1		$4.1 \times 10^7 \text{ M}^{-1}$	-----	$5.1 \times 10^8 \text{ M}^{-1}$	1.0
2 + 2		$9.6 \times 10^7 \text{ M}^{-1}$	$5.4 \times 10^8 \text{ M}^{-1}$	-----	1.0
2 + 1		$4.2 \times 10^8 \text{ M}^{-1}$	$4.6 \times 10^8 \text{ M}^{-1}$	$5.2 \times 10^8 \text{ M}^{-1}$	1.0
18 + 18		-----	-----	$2.7 \times 10^7 \text{ M}^{-1}$.05
17 + 17		$5.1 \times 10^7 \text{ M}^{-1}$	-----	$6.7 \times 10^8 \text{ M}^{-1}$	1.3
8 + 8		$1.2 \times 10^7 \text{ M}^{-1}$	-----	$1.7 \times 10^9 \text{ M}^{-1}$	3.3
12 + 12		$8.5 \times 10^7 \text{ M}^{-1}$	-----	$6.6 \times 10^8 \text{ M}^{-1}$	1.3
16 + 16		$4.0 \times 10^8 \text{ M}^{-1}$	$1.3 \times 10^8 \text{ M}^{-1}$	$6.5 \times 10^9 \text{ M}^{-1}$	11.0
21 + 20		$2.0 \times 10^7 \text{ M}^{-1}$	$2.0 \times 10^7 \text{ M}^{-1}$	$3.4 \times 10^7 \text{ M}^{-1}$	0.065
3 + 3		-----	-----	$2.8 \times 10^7 \text{ M}^{-1}$	0.05
15 + 14		$3.7 \times 10^9 \text{ M}^{-1}$	$2.0 \times 10^9 \text{ M}^{-1}$	$6.7 \times 10^9 \text{ M}^{-1}$	12.9

Table 2 (continued): Equilibrium Association Constants*

PA #	Polyamide	5'-TGGTACA-3'	5'-TGGTCCA-3'	5'-TGTTACA-3'	$\Delta K_a(\text{parent})$
19 + 14		$1.1 \times 10^9 \text{ M}^{-1}$	$2.5 \times 10^8 \text{ M}^{-1}$	$5.7 \times 10^9 \text{ M}^{-1}$	2.4
21 + 14		$1.0 \times 10^9 \text{ M}^{-1}$	$2.6 \times 10^8 \text{ M}^{-1}$	$7.6 \times 10^9 \text{ M}^{-1}$	2.4
19 + 16		$3.5 \times 10^8 \text{ M}^{-1}$	$1.0 \times 10^8 \text{ M}^{-1}$	$2.1 \times 10^9 \text{ M}^{-1}$	0.83
21 + 16		$3.4 \times 10^8 \text{ M}^{-1}$	$9.8 \times 10^7 \text{ M}^{-1}$	$2.3 \times 10^9 \text{ M}^{-1}$	0.83
13 + 18		$2.1 \times 10^8 \text{ M}^{-1}$	$1.5 \times 10^9 \text{ M}^{-1}$	$1.8 \times 10^8 \text{ M}^{-1}$	0.5
13 + 21		$2.1 \times 10^8 \text{ M}^{-1}$	$1.5 \times 10^9 \text{ M}^{-1}$	$2.0 \times 10^8 \text{ M}^{-1}$	0.5
13 + 22		$9.8 \times 10^7 \text{ M}^{-1}$	$1.46 \times 10^9 \text{ M}^{-1}$	$2.4 \times 10^8 \text{ M}^{-1}$	0.23
11 + 7		$6.5 \times 10^8 \text{ M}^{-1}$	$9.5 \times 10^8 \text{ M}^{-1}$	$4.1 \times 10^8 \text{ M}^{-1}$	1.5
11 + 12		$1.2 \times 10^9 \text{ M}^{-1}$	$1.3 \times 10^9 \text{ M}^{-1}$	$6.6 \times 10^9 \text{ M}^{-1}$	2.9
7 + 6		$1.0 \times 10^8 \text{ M}^{-1}$	$1.8 \times 10^8 \text{ M}^{-1}$	$2.2 \times 10^8 \text{ M}^{-1}$	0.23

*Equilibrium association constants are the mean values obtained from three quantitative DNase I footprinting experiments. The standard deviation for each data point is less than 10% of the value reported. Assays were carried out as reported in the text. Dashed lines indicated no binding at that site. Left column; Polyamide number (Figure 4.7) – First number corresponds to the top polyamide pictured in column 2. #: Where multiple match sites are available (heterodimer assays), the relative affinity given the ratio of binding affinities of the functionalized polyamides listed relative to the binding affinity of the unfunctionalized parent polyamides (PA1 + PA2) on the heterodimer site (5'-aTGGTACA-3').

propylguanidyl (**PA16**) and ethylamino (**PA13**) side chains bind with slightly lower affinity when paired with the aromatic side chains.

The putative hydrogen-bonding interactions (**PA12** homodimer, **PA6** with **PA7**, **PA12** with **PA9**, and **PA10** with **PA7**) give binding affinities that were quite varied. With respect to the unfunctionalized polyamides, ImPyPy(2Am)PyPy- β -Dp (ethylamido side chain: **PA12**) homodimerically paired does not differ in affinity from the parent polyamides. In contrast, **PA12** paired with the ImImDsPyPy- β -Dp (**PA9**) gives a 3-fold increase in affinity over the unmodified system, binding with a K_a of 1.2 nM^{-1} . Both the primary amide (**PA6** (ImPy(Am)PyPyPy- β -Dp) with **PA7** (ImImPyPy(Am)Py- β -Dp)) homodimer and the primary amide (**PA7**) with ImDsPyPyPy- β -Dp (hydrogen side chain: **PA10**) heterodimer fail to increase polyamide affinity.

In order to assess the specificity of the isobutyl interaction, ImImPyPy(iBu)Py- β -Dp (**PA5**) was synthesized and footprinted with **PA3**. As shown in Figure 4.9, when the isobutyl side chains are paired against the standard methyl group, and separated from each other by one residue, over 70% of the affinity loss incurred by the isobutyl pairing is rescued. Furthermore, when the two isobutyl groups are separated by two residues, another 15% of the binding affinity is recovered.

Because the isobutyl functional group showed a pair-specific destabilizing effect, Im(iBu)DsPyPyPy(iBu)- β -Dp (**PA23**) and ImImPy(iBu)DsPy- β -Dp (**PA24**) were synthesized and probed for their ability to favor the heterodimeric binding motif over either of the two homodimeric binding motifs. Because each isobutyl group contributes a two-fold, non-specific reduction in affinity, the Des-methyl pyrrole monomer was incorporated in order to non-specifically boost the affinity of the polyamides. As shown

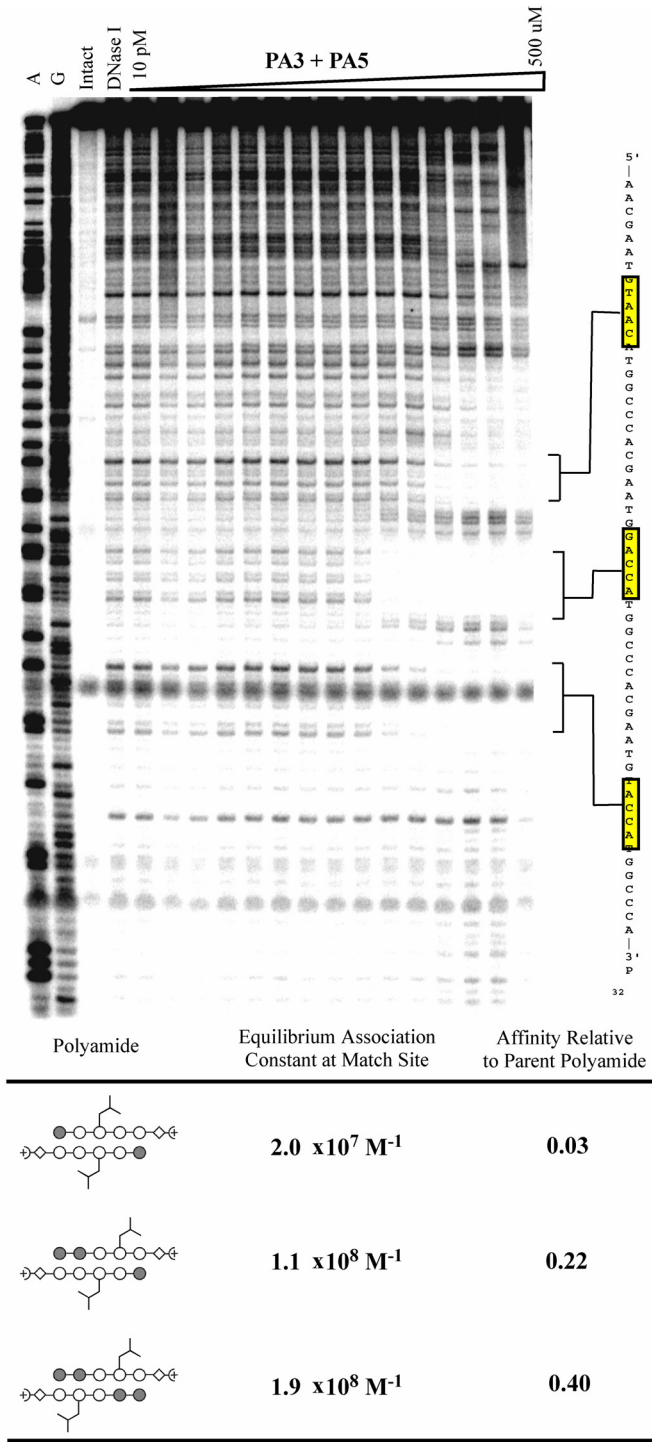


Figure 4.9. Top: Quantitative DNase footprinting experiment with ImPyPy(iBu)PyPy- β -Dp (**PA3**) and ImImPyPy(iBu)Py- β -Dp (**PA5**) on the 3'- 32 P-labeled restriction fragment pDHN2. Gel lanes from left to right: A reaction, G reaction, intact DNA, DNase I standard, DNase digestion products in the presence of 10 pM, 20 pM, 50 pM, 100 pM, 200 pM, 500 pM, 1 nM, 2 nM, 5 nM, 10 nM, 20 nM, 50 nM, 100 nM, 200 nM, 500 nM polyamide. Bottom: Data table illustrating the binding affinities at each of the three match sites.

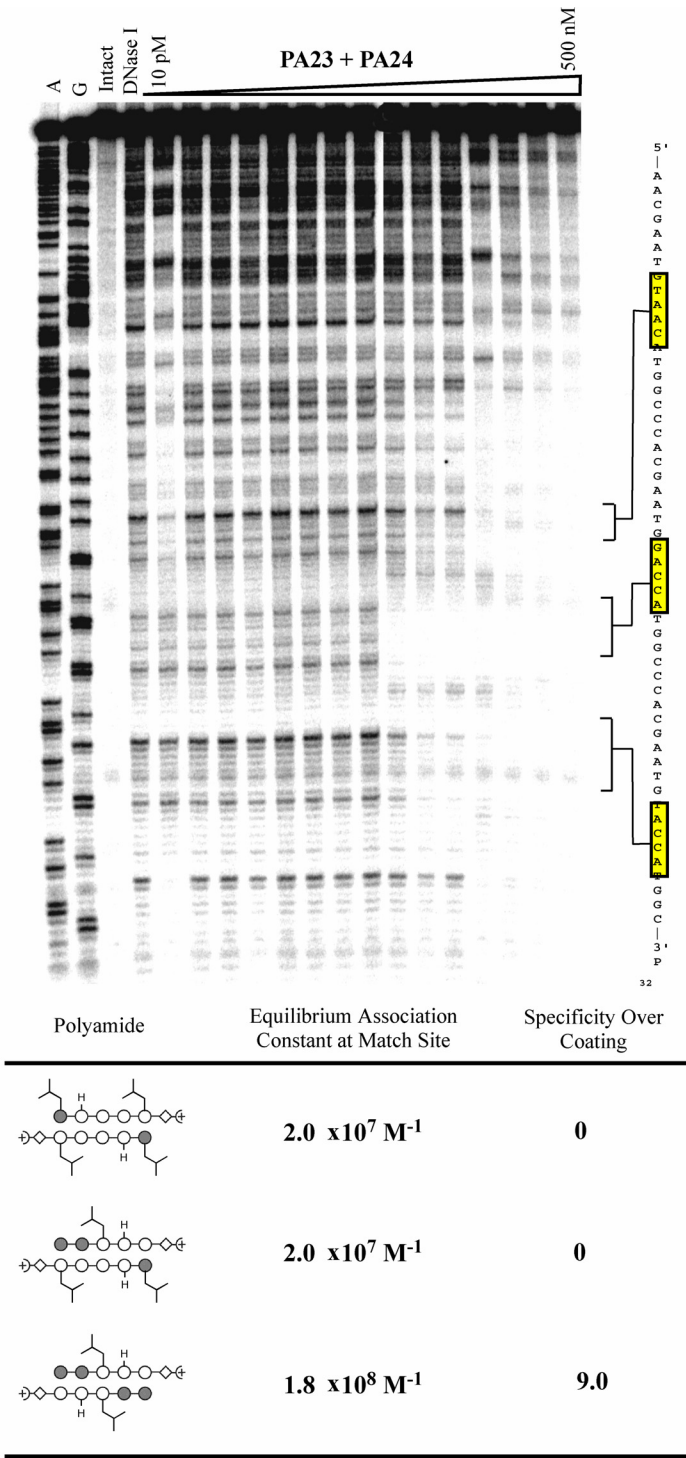


Figure 4.10. Top: Quantitative DNase footprinting experiment with Im(iBu)PyPyPyPy(iBu)- β -Dp (**PA23**) and ImImPy(iBu)PyPy- β -Dp (**PA24**) on the 3'- ^{32}P -labeled restriction fragment pDHN2. Gel lanes from left to right: A reaction, G reaction, intact DNA, DNase I standard, DNase digestion products in the presence of 10 pM, 20 pM, 50 pM, 100 pM, 200 pM, 500 pM, 1 nM, 2 nM, 5 nM, 10 nM, 20 nM, 50 nM, 100 nM, 200 nM, 500 nM polyamide. Bottom: Data table illustrating the binding affinities at each of the three match sites.

in Figure 4.10, these polyamides bind each of the three designed sites with affinities below the parent polyamides. **PA23**, which contains only one isobutyl group, can still be seen to bind at its match site with an affinity of $1.8 \times 10^8 \text{ M}^{-1}$. No binding can be seen at either the one-imidazole or heterodimer match sites. Instead, protection from DNase I cleavage is incurred along the entire oligonucleotide (a phenomenon dubbed “coating”) at concentrations as low as 50 nM. When **PA23** and **PA24** are footprinted separately, the coating is seen only when the DNA is equilibrated with **PA24**.

Discussion.

The results of the quantitative DNase I footprinting analysis have shown that the issue of hetero- versus homodimer formation can be controlled by non-covalent negative interactions. An example of this is the isobutyl side chain. When this side chain is paired across from itself in a DNA:polyamide complex, the polyamide affinity for the DNA is compromised 16-fold. By moving the sterically bulky groups apart by two residues, the binding affinity loss is rescued. Modeling data¹⁵ for the isobutyl side chain homodimer pairing indicates that the bond between the pyrrole nitrogen and the isobutyl methylene group would need to bend 14° away from the plane of the pyrrole ring for the two bulky groups to fit within the minor groove together. Thus, the modeling data correlate well with the experimental footprinting data. When multiple isobutyl groups are placed on a single 5-ring polyamide (as in **PA24**), the polyamide loses its ability to discriminate DNA sequence and coats the oligonucleotide. One hypothesis to explain these results is that placement of multiple hydrophobic groups on a polyamide designed to bind in the hydrophobic minor groove causes favorable desolvation energetics to outcompete the

energy loss of binding the polyamide non-specifically to DNA. Thus, the polyamide is forced into the hydrophobic minor groove even if it is required to tolerate a mismatch at that site. Both the benzyl and ethyl benzyl side chains exhibit similar specific loss of affinity as the isobutyl side chain when homodimerically paired. Perhaps these side chains can be used as negative control elements without the unwanted coating behavior exhibited by polyamides with multiple isobutyl functionalities.

One interesting result is that the benzyl group (**PA20**) gave a significantly reduced binding affinity while the isosteric pentafluorobenzyl group (**PA17**) did not alter affinity. Modeling data¹⁶ show that the benzyl group is unable to lie in the same plane as the polyamide without the benzyl 2H sterically clashing with the backbone carbonyl group of the polyamide chain. Two of these rotated benzyl groups cannot fit within the minor groove without disfavorable steric interactions when paired. The higher affinity of the pentafluorobenzyl group may be attributable to its quadrupole. Because the five electronegative fluorine atoms pull electron density out of the aromatic ring, the π cloud is significantly electropositive. The destabilizing steric effects of the ring/ring pairing may be balanced by a stabilizing electrostatic interaction between this electropositive moiety and the negatively charged phosphodiester backbone.

Unfortunately, non-covalent, positively interacting side chains fail to exhibit specific increases in dimer affinity. Each of the side chains carrying a positive charge shows an increase in affinity when incorporated into polyamides. However, the observed increase is not specific to a side chain/side chain pairing. The positive charge on the side chain is able to form a favorable electrostatic interaction with the negatively charged phosphodiester backbone of the DNA. The propylamino and guanidyl side chains give

larger binding affinity increases than the ethylamino-functionalized polyamide. This suggests that the longer chain length is more optimal for interacting with the phosphodiester backbone. Modeling shows that the ethylamino group lacks the chain length necessary to reach the DNA backbone, and therefore, would be an ideal candidate to participate in specific cation/ π interactions while not participating in non-specific, associative DNA contacts. While two ethylamino groups present in a dimeric polyamide/DNA complex show only a modest 3-fold increase in affinity (due to non-specific electrostatic interactions with the DNA), pair-wise interactions with each of the aromatic side chains fail to exhibit affinity increases specific to the putative cation/ π pairing.

Likewise, hydrogen bonding interactions between the primary amide groups and the N1 proton of pyrrole fail to impart specific affinity increases. Incorporation of the des-methyl pyrrole ring into the polyamide stabilizes the complex with DNA 3-5-fold. Thus, the apparent affinity increases seen when the des-methyl pyrrole is paired with the amide side chains are non-specific, and a result of the incorporation of the des-methyl ring, not a specific hydrogen bonding interaction.

Each of the non-covalent associative forces tested here have been shown to aid in protein folding and association. However, in proteins, these interacting side chains are removed from a protic solvent environment and interaction takes place inside the greasy protein interior, where their effects are increased. One hypothesis for the failure of non-covalent associative forces to incur specificity in this polyamide-based system is that the spatial area above the minor groove of DNA where the interactions tested here take place is a water-accessible area. This makes the associative interactions weaker due to water

solvation. An alternative hypothesis is that the polyamide/DNA complex is a flexible and dynamic complex, and that one or two additional weakly associative forces on the backbone are not enough to overcome the inherent motion of the polyamide strands with respect to the DNA. In conclusion, while non-covalent associative forces fail to specify for one binding mode, side chains such as the bulky isobutyl group are able to cause a specific destabilization of DNA binding, which may be used to refine the sequence space targeted by dimeric polyamide/DNA complexes.

Materials and Methods.

Dicyclohexylcarbodiimide (DCC), hydroxybezotriazole (HOBT), 2-(1H-benzotriazole-1-yl)-1,1,3,3,-tetramethyluronium hexafluorophosphate (HBTU), and 0.6 mmol/g Boc- β -Ala-Pam-Resin were purchased from Peptides International.

2-Bromoethyl acetamide was purchased from TCI America. All other chemicals were purchased from Aldrich Chemicals and used without further purification. Anhydrous dimethylformamide (DMF), N-methylpyrrolidone (NMP), N,N-dimethylpropylamine (Dp), and N,N-diisopropylethylamine (DIEA) were purchased from Aldrich Chemicals and stored over 3 Å molecular sieves. All other solvents were purchased from EM Sciences and were reagent-grade. Deuterated NMR solvents were purchased from Cambridge Isotopes.

^1H NMR spectra were recorded on a 300 MHz General Electric–QE NMR spectrometer with chemical shifts reported in parts per million relative to the residual solvent peak. UV spectra were recorded in water on a Hewlett-Packard Model 8452A diode array spectrophotometer. Matrix-assisted, LASER desorption/ionization time of

flight mass spectrometry was performed on a Voyager DE Pro Spectrometer. Electrospray ionization (E/I) mass spectrometry was performed at the Protein and Peptide Microanalytical Facility at the California Institute of Technology. HPLC analysis was performed on a Beckman Gold System using a Rainen C₁₈, microsorb Mv, 5 μ m, 300 x 4.6 mm reversed-phase column in a 0.1%(wt/v) TFA aqueous solution with acetonitrile as eluent at a flow rate of 1.0 mL/min and a gradient elution of 1.25% acetonitrile/min. Preparative HPLC was performed on a Beckman Instrument using a Waters DeltaPak 25 x 100 mm, 100 μ m C₁₈ reversed-phase column with a guard. The solvent was 0.1% (wt/v) aqueous TFA at 8.0 mL/min with 0.25%/min acetonitrile as the eluent. Gels were imaged using a Molecular Dynamics 400S PhosphorImager.

Restriction endonucleases, deoxyribonucleotide triphosphates, and glycogen were purchased from Boeringher-Mannheim. Sequenase was obtained from Amersham Life Sciences. DNase I and deproteinized calf thymus DNA were purchased from Pharmacia Biotech. [α -³²P]-Thymidine-5'-triphosphate (≥ 3000 Ci/mmol) and [α -³²P]-Deoxyadenosine-5'-triphosphate (≥ 6000 Ci/mmol) were purchased from New England Nucleosides. Water was used from a Millipore Milli-Q purification system. All buffer reagents were purchased from Fluka Biochemika Microselect. All buffers were sterilized by filtration through Nalgene 0.2 μ m cellulose nitrate filtration devices.

Monomer Synthesis.

1,2,3-Benzotriazol-1-yl 4-[(tert-butoxy)carbonylamino]-1-methylpyrrole-2-carboxylic acid (Boc-Py-OBt), 4[(tert-butoxy)carbonylamino]-1-methylimidazole-2-carboxylic acid (Boc-Im-OH), imidazole-2-carboxylic acid (Im-OH), 4[(tert-

butoxy)carbonylamino]-pyrrole-2-carboxylic acid (Boc-Ds-OH, **7j**), and 4-[(tert-butoxy)carbonylamino]-1-[3-(1,3-dioxoisindolin-2-yl)propyl]pyrrole-2-carboxylic acid (Boc-Py(3Ph)-OH, **7a**) were synthesized according to published procedures.¹¹⁻¹³ 4-[(tert-butoxy)carbonylamino]-1benzylpyrrole-2-carboxylic acid (Boc-Py(Bz)-OH, **7i**) was prepared by Nick Wurtz (unpublished results).

General procedure for alkylation of 3,3-dimethyl-3-silabutyl 4-nitropyrrole-2-carboxylate (2) and ethyl 4-nitropyrrole-2-carboxylate (1) for compounds 5a, d–f, h, k

To a solution of the 4-nitropyrrole-2-carboxylate (1.0 mmol) in 25 mL acetone dried over K_2CO_3 was added powdered K_2CO_3 (2.0 mmol). This suspension was stirred at rt for 30 min. The appropriate alkyl bromide (1.2 mmol) was then added, followed by tetrabutylammonium iodide (0.2 mmol). The reaction was refluxed until completion as determined by TLC (1–24h). The reaction was cooled and the acetone evaporated *in vacuo*. The residue was taken up in water (50 mL) and extracted with ethyl acetate (2 x 100 mL). The combined organic layer was dried (sodium sulfate) and concentrated *in vacuo*. The residue was then chromatographed in the appropriate solvent conditions to yield the pure 1-alkylated 4-nitropyrrole-2-carboxylate.

General procedure for alkylation of 3,3-dimethyl-3-silabutyl 4-[(tert-butyl)carbonylamino]pyrrole-2-carboxylate (4) and ethyl 4-[(tert-butyl)carbonylamino]pyrrole-2-carboxylate (3) for compounds 6b, c

To a solution of the 4-[(tert-butoxy)carbonylamino]pyrrole-2-carboxylate (1.0 mmol) in 25 mL acetone dried over K_2CO_3 was added powdered K_2CO_3 (2.0 mmol). This suspension was stirred at rt for 30 min. The appropriate alkyl bromide (1.2 mmol) was then added, followed by tetrabutylammonium iodide (0.2 mmol). The reaction was refluxed until completion as determined by TLC (1-24h). The reaction was cooled and the acetone evaporated *in vacuo*. The residue was taken up in water (50 mL) and extracted with ethyl acetate (2 x 100 mL). The combined organic layer was dried (sodium sulfate) and concentrated *in vacuo*. The residue was then chromatographed in the appropriate solvent conditions to yield the pure 1-alkylated 4-[(tert-butoxy)carbonylamino]-2-carboxylate.

General procedure for reduction and boc-protection of alkylated 3,3-dimethyl-3-silabutyl 4-nitropyrrole-2-carboxylate and ethyl 4-nitropyrrole-2-carboxylate derivatives (5a,d-f,h,k) for compounds 6a, d-f, h, k

To a solution of the 4-nitropyrrole 2-carboxylate derivative (1.0 mmol) in 25 mL ethyl acetate was added 10% Pd/C (20% by wt). The mixture was stirred vigorously under 400 psi of hydrogen for 1–12 h. When complete, the reaction was filtered through Celite, and the Celite washed with ethyl acetate (3 x 10 mL). The filtrates were combined and Boc anhydride (1.1 mmol) was added, followed by 1M $NaHCO_3$ (50 mL). The biphasic reaction mixture was stirred vigorously at rt until completion as determined by TLC. The layers were separated and the organic layer washed with 10% citric acid (2 x 50 mL) followed by brine (2 x 50 mL). The organic layer was dried (sodium sulfate) and concentrated *in vacuo*. The residue was then column chromatographed in the appropriate

solvent system to yield the pure 4-[(tert-butoxy)carbonylamino]pyrrole-2-carboxylate derivative.

General procedure for the hydrolysis of ethyl esters 6c, d, f, h, k

To a solution of the 4-[(tert-butoxy)carbonylamino]pyrrole-2-carboxylate derivative (1.0 mmol) in 10 mL ethanol was added 10 mL of a 5.0 M solution of sodium hydroxide. The reaction was stirred at rt until completion as determined by TLC. The ethanol was removed *in vacuo* and the aqueous layer acidified with 10% H₂SO₄ to pH 3. The carboxylic acid product was then extracted with ethyl acetate (2 x 25 mL). The combined organic layer was dried (sodium sulfate) and concentrated *in vacuo* to yield the pure product.

General procedure for the deprotection of trimethylsilylethyl esters 6a, b, e

A solution of the 3,3-dimethyl-3-silabutyl 4-[(tert-butoxy)carbonylamino]pyrrole-2-carboxylate derivative (1.0 mmol) in 5 mL anhydrous THF under argon was cooled to 0 °C on an ice bath. A 2.0 M solution of TBAF in THF (0.5 mL) was added drop-wise to the cooled reaction mixture. The reaction was allowed to warm slowly to room temp where it was stirred overnight under argon. The reaction was then quenched with the addition of 1 mL 10% citric acid and cooled to -20 °C where the pure carboxylic acid crystallized out. The crystalline product was filtered and washed with cold hexanes to yield the pure product.

3,3-dimethyl-3-silabutyl-4-[(tert-butoxy)carbonylamino]-1-[(2,3,4,5,6-pentafluorophenyl)methyl]pyrrole-2-carboxylate (6b)

From 2.0 g (7.8 mmol) **4** and 2,3,4,5,6-pentafluorobenzyl bromide (2.04 g, 7.8 mmol) was yielded 3.2 g (88%) of **6b** as a pale brown solid after flash chromatography in 1:1 hexanes/ethyl acetate. TLC (ethyl acetate) R_f 0.85 ^1H NMR(DMSO- d_6) δ 9.20 (s, 1H), 7.17 (s, 1H), 6.60 (s, 1H), 5.68 (s, 2H), 4.23 (t, 2H, $J=8.4$), 1.42 (s, 9H), 0.95 (t, 2H, $J=8.4$), 0.00 (s, 9H). E/I MS m/e 507.4 (M+H) (506.17 calcd. for $\text{C}_{22}\text{H}_{27}\text{F}_5\text{N}_2\text{O}_4\text{Si}$).

4-[(tert-butoxy)carbonylamino]-1-[(2,3,4,5,6-pentafluorophenyl)methyl]pyrrole-2-carboxylic acid (Boc-Py(5F)-OH) (7b)

From 3.0 g (5.94 mmol) **6b** was yielded 2.1 g (88%) of **7b** as a pale brown powder. TLC (ethyl acetate) R_f 0.05 ^1H NMR(DMSO- d_6) δ 12.22 (bs, 1H) 9.16 (s, 1H), 7.09 (s, 1H), 6.59 (s, 1H), 5.65 (s, 2H), 1.41 (s, 9H). E/I MS m/e 405.2(M-H)(406.10 calcd. for $\text{C}_{17}\text{H}_{15}\text{F}_5\text{N}_2\text{O}_4$).

Ethyl 4-[(tert-butoxy)carbonylamino]-1-(2-phenylethyl)pyrrole-2-carboxylate (6c)

From 6.0g (23.7 mmol) **3** and bromoethyl benzene (5.24g, 28.3 mmol) was yielded 3.6 g (42%) **6c** after flash chromatography in 3:17 ethyl acetate/hexanes as a clear oil. TLC (1:9 hexanes/ethyl acetate) R_f 0.17 ^1H NMR(DMSO- d_6) δ 9.11 (s, 1H), 7.30 (m, 1H), 7.26 (d, 2H, $J=6.9$), 7.19 (d, 2H, $J=6.9$), 7.11 (s, 1H), 6.64 (s, 1H), 4.39 (t, 2H, $J=8.1$), 4.17 (q, 2H, $J=7.2$), 2.90 (t, 2H, $J=7.4$), 1.42 (s, 9H), 1.24 (t, 2H, $J=7.2$). E/I MS m/e 359.3 (M+H) (359.19 calcd. for $\text{C}_{20}\text{H}_{26}\text{N}_2\text{O}_4$).

4-[(tert-butoxy)carbonylamino]-1-(2-phenylethyl)pyrrole-2-carboxylic acid (Boc-Py(2Bz)-OH) (7c)

From 1.5 g (4.2 mmol) **6c** was yielded 1.1 g (79%) of **7c** as a white powder. TLC (ethyl acetate) R_f 0.05 ^1H NMR(DMSO- d_6) δ 8.89 (s, 1H), 7.26 (m, 5H), 6.85 (s, 1H), 6.36 (s, 1H), 4.42 (t, 2H, $J=7.8$), 2.90 (t, 2H, $J=7.6$), 1.41 (s, 9H). E/I MS m/e 329.1 (M-H) (330.16 calcd. for $\text{C}_{18}\text{H}_{22}\text{N}_2\text{O}_4$).

Ethyl 4-nitro-1-(2-carbamoylethyl)pyrrole-2-carboxylate (5d)

From 2.5 g (13.6 mmol) **1** and 2-bromoethyl acetamide (2.27 g, 15 mmol) was yielded 2.8 g (81%) of **5d** after flash chromatography in 2:1 ethyl acetate/hexanes as a white powder. TLC (2:1 hexanes/ethyl acetate) R_f 0.22 ^1H NMR(DMSO- d_6) δ 8.13 (d, 1H, $J=1.8$), 7.35 (s, 1H), 7.32 (d, 1H, $J=1.8$), 6.92 (s, 1H), 4.52 (t, 2H, $J=6.9$), 4.32 (q, 2H, $J=7.2$), 2.59 (t, 2H, $J=6.6$), 1.29 (t, 2H, $J=7.5$). E/I MS m/e 256.4 (M+H) (255.09 calcd. for $\text{C}_{10}\text{H}_{13}\text{N}_3\text{O}_5$).

Ethyl 4-[(tert-butoxy)carbonylamino]-1-(2-carbamoylethyl)pyrrole-2-carboxylate (6d)

From 2.5 g (11 mmol) **5d** was yielded 2.14 g (60%) **6d** after flash chromatography in 100% ethyl acetate as a white powder. TLC (ethyl acetate) R_f 0.71 ^1H NMR(DMSO- d_6) δ 9.12 (s, 1H), 7.32 (s, 1H), 7.04 (s, 1H), 6.81 (s, 1H), 6.60 (s, 1H), 4.39 (t, 2H, $J=6.6$), 4.18 (q, 2H, $J=7.4$), 2.42 (t, 2H, $J=6.6$), 1.41 (s, 9H), 1.27 (t, 2H, $J=7.4$). E/I MS m/e 326.2 (M+H) (325.16 calcd. for $\text{C}_{15}\text{H}_{23}\text{N}_3\text{O}_5$).

4-[(tert-butoxy)carbonylamino]-1-(2-carbamoylethyl)pyrrole-2-carboxylic acid (Boc-Py(2Am)-OH) (7d)

From 600 mg (1.85 mmol) **6d** was yielded 550 mg (97%) **7d** as a white powder. TLC (ethyl acetate) R_f 0.05 ^1H NMR(DMSO- d_6) δ 9.05 (s, 1H), 7.30 (s, 1H), 7.03 (s, 1H), 6.82 (s, 1H), 6.57 (s, 1H), 4.36 (t, 2H, $J=6.9$), 2.45 (t, 2H, $J=6.8$), 1.42 (s, 9H). E/I MS m/e 296.1 (M-H) (297.13 calcd. for $\text{C}_{13}\text{H}_{19}\text{N}_3\text{O}_5$).

3,3-dimethyl-3-silabutyl-4-nitro-1-[2-(1,3-dioxoisindolin-2-yl)ethyl]pyrrole-2-carboxylate (5e)

2 (2.0 g, 7.8 mmol) and 2-bromoethyl phthalimide (2.39 g, 9.37 mmol) were combined in acetone along with powdered K_2CO_3 (1.61 g, 11.7 mmol) and tetrabutylammonium iodide (576 mg, 1.5 mmol) and stirred at 40 °C for 48 h. Every 12 h, an additional 0.5 equivalents of 2-bromoethyl phthalimide (994 mg, 3.4 mmol) was added. 3.0 g (90%) **5e** was isolated after the standard workup and flash chromatography in 4:1 hexanes/ethyl acetate as a clear oil. TLC (6:1 hexanes/ethyl acetate) R_f 0.12 ^1H NMR(DMSO- d_6) δ 8.38 (d, 1H, $J=2.4$), 7.84 (m, 4H), 7.22 (d, 1H, $J=2.4$), 4.64 (t, 2H, $J=6.6$), 4.04 (t, 2H, $J=7.4$), 3.96 (t, 2H, $J=6.6$), 0.79 (t, 2H, $J=7.4$), 0.00 (s, 9H). E/I MS m/e 430.5 (M+H) (429.14 calcd. for $\text{C}_{20}\text{H}_{23}\text{N}_3\text{O}_6\text{Si}$).

3,3-dimethyl-3-silabutyl 4-[(tert-butoxy)carbonylamino]-1-[2-(1,3-dioxoisindolin-2-yl)ethyl]pyrrole-2-carboxylate (6e)

From 1.25 g (2.9 mmol) **5e** was isolated 1.3 g (90%) **6e** after flash chromatography in 5:2 hexanes/ethyl acetate. TLC (1:1 hexanes/ethyl acetate) R_f 0.86 ^1H NMR(DMSO- d_6) δ 9.10 (s, 1H), 7.83 (m, 4H), 7.04 (s, 1H), 6.56 (s, 1H), 4.51 (t, 2H, $J=6.6$), 3.93 (t, 2H,

J=6.6), 3.87 (t, 2H, J=7.4), 1.42(s, 9H), 0.76 (t, 2H, J=7.4), 0.00 (s, 9H). E/I MS m/e 500.1 (M+H) (499.21 calcd. for C₂₅H₃₃N₃O₆Si).

4-[(tert-butoxy)carbonylamino]-1-[2-(1,3-dioxoisindolin-2-yl)ethyl]pyrrole-2-carboxylic acid (Boc-Py(2P)-OH) (7e)

From 1.15 g (2.3 mmol) **6e** was yielded 900 mg (98%) **7e** as a white powder. TLC (2:1 hexanes/ethyl acetate) R_f 0.05 ¹H NMR(DMSO-*d*₆) δ 12.05 (bs, 1H), 8.98 (s, 1H), 7.79 (m, 4H), 6.88 (s, 1H), 6.51 (s, 1H), 4.44 (t, 2H, J=6.6), 3.87 (t, 2H, J=6.6), 1.36 (s, 9H). E/I MS m/e 398.6 (M-H) (399.14 calcd. for C₂₀H₂₁N₃O₆).

Ethyl 4-nitro-1-(2-methylpropyl)pyrrole-2-carboxylate (5f)

From 6.0 g (32.6 mmol) **1** and 1-bromo-2-methylpropane (5.8 g, 42.4 mmol) was yielded 7.14 g (91%) **5f** as a yellow solid. TLC (3:2 hexanes/ethyl acetate) R_f 0.90 ¹H NMR(DMSO-*d*₆) δ. E/I MS m/e 241.1 (M+H) (240.11 calcd. for C₁₁H₁₆N₂O₄).

Ethyl 4-[(tert-butoxy)carbonylamino]-1-(2-methylpropyl)pyrrole-2-carboxylate (6f)

From 3.5 g (14.5 mmol) **5f** was yielded 4.1 g (91%) **6f** after flash chromatography in 5:2 hexanes/ethyl acetate as an off-white solid. TLC (3:2 hexanes/ethyl acetate) R_f 0.80 ¹H NMR(DMSO-*d*₆) δ 9.17 (s, 1H), 7.06 (s, 1H), 6.64 (s, 1H), 4.16 (q, 2H, J=6.0), 4.01 (d, 2H, J=7.2), 1.91 (m, 1H), 1.42 (s, 9H), 1.23 (t, 2H, J=5.9), 0.77 (d, 6H, J=7.2). E/I MS m/e 310.9 (M+H) (310.19 calcd. for C₁₆H₂₆N₂O₄).

4-[(tert-butoxy)carbonylamino]-1-(2-methylpropyl)pyrrole-2-carboxylic acid (Boc-Py(iBu)-OH) (7f)

From 1.24 g (3.99 mmol) **6f** was yielded 980 mg (88%) **7f** as a white solid. TLC (3:2 hexanes/ethyl acetate) R_f 0.05 ^1H NMR(DMSO- d_6) δ 9.03 (s, 1H), 7.00 (s, 1H), 6.56 (s, 1H), 4.03 (d, 2H, $J=6.0$), 1.91 (m, 1H), 1.41 (s, 9H), 0.78 (d, 6H, $J=7.2$). E/I MS m/e 281.3 (M-H) (282.16 calcd. for $\text{C}_{14}\text{H}_{22}\text{N}_2\text{O}_4$).

Tert-butyl 3-(2-[4-nitro-2-(ethoxycarbonyl)pyrrolyl]ethyl)indolecarboxylate (5k)

From 300 mg (1.63 mmol) **1** and tert-butyl 3-(bromomethyl)indolecarboxylate (554 mg, 1.79 mmol) was yielded 485 mg (73%) **5k** after flash chromatography in 6:1 hexanes/ethyl acetate as a pale yellow powder. TLC (2:1 hexanes/ethyl acetate) R_f 0.95 ^1H NMR(DMSO- d_6) δ 8.405 (d, 1H, $J=2.1$), 8.03 (d, 1H, $J=8.4$), 7.69 (s, 1H), 7.63 (d, 1H, $J=8.4$), 7.34 (d, 1H, $J=2.1$), 7.25 (m, 2H), 5.74 (s, 2H), 4.27 (q, 2H, $J=7.2$), 1.60(s, 9H), 1.27 (t, 2H, $J=7.2$). E/I MS m/e 414.2 (M+H) (413.16 calcd. for $\text{C}_{21}\text{H}_{23}\text{N}_3\text{O}_6$).

Tert-butyl-3-(2-{4-[(tert-butoxy)carbonylamino]-2-

(ethoxycarbonyl)pyrrolyl)ethyl)indolecarboxylate (6k)

From 450 mg (1.09 mmol) **5k** was yielded 450 mg (86%) **6k** after flash chromatography in 6:1 hexanes/ethyl acetate as a pale yellow solid. TLC (5:1 hexanes/ethyl acetate) R_f 0.37 ^1H NMR(DMSO- d_6) δ 9.11 (s, 1H), 8.01 (d, 1H, $J=2.4$), 7.55 (s, 1H), 7.54 (d, 1H, $J=9.0$), 7.32 (t, 1H, $J=8.1$), 7.21 (s, 1H), 7.20 (m, 1H), 6.65 (s, 1H), 5.62 (s, 2H), 4.20 (q, 2H, $J=7.2$), 1.60(s, 9H), 1.38 (s, 9H), 1.24 (t, 2H, $J=6.9$). E/I MS m/e 484.3 (M+H) (483.24 calcd. for $\text{C}_{26}\text{H}_{33}\text{N}_3\text{O}_6$).

4-[(tert-butoxy)carbonylamino]-1-(2-indole-2-ylmethyl)pyrrole-2-carboxylic

acid (Boc-Py(In)-OH) (7g)

From 400 mg (0.83 mmol) **6k** was yielded 286 mg (97%) **7g** as a pale yellow solid. TLC (7:1 hexanes/ethyl acetate) R_f 0.10 ^1H NMR(DMSO- d_6) δ 11.03 (s, 1H), 9.11 (s, 1H), 7.49 (t, 1H, $J=6.6$), 7.35 (d, 1H, $J=8.1$), 7.33 (s, 1H), 7.06 (s, 1H), 7.03 (m, 1H), 6.95 (t, 1H, $J=7.2$), 6.59 (s, 1H), 5.61 (s, 2H), 1.37 (s, 9H). E/I MS m/e 354.5 (M-H) (355.15 calcd. for $\text{C}_{19}\text{H}_{21}\text{N}_3\text{O}_4$).

Ethyl 4-nitro-1-(cyanomethyl)pyrrole-2-carboxylate (5h)

Sodium Hydride (60% dispersion in mineral oil, 304 mg, 7.6 mmol) was dissolved in 3 mL anhydrous DMF and stirred under argon at 0 °C. **1** (1.0 g, 5.43 mmol) dissolved in 6 mL anhydrous DMF was then added drop wise and the solution stirred for 30 min. Bromoacetonitrile (1.15 g, 9.77 mmol) was then added drop wise to the reaction mixture allowed to warm to room temperature, where it was stirred overnight. The reaction mixture was poured into water (50 ml) and the product extracted with ethyl acetate (2 x 100 mL). The combined organic layer was then washed with brine (2 x 50 mL), dried over sodium sulfate, and concentrated *in vacuo*. The residue was then flash chromatographed in 1:1 ethyl acetate/hexanes to yield 1.07 g (89%) **5h** as a pale yellow oil. TLC (1:1 hexanes/ethyl acetate) R_f 0.60 ^1H NMR(DMSO- d_6) δ 8.40 (d, 1H, $J=2.4$), 7.41 (d, 1H, $J=2.4$), 5.50 (s, 2H), 4.31 (q, 2H, $J=6.9$), 1.30 (t, 2H, $J=6.9$). E/I MS m/e 224.0 (M+H) (223.06 calcd. for $\text{C}_9\text{H}_9\text{N}_3\text{O}_4$).

Ethyl 4-[(tert-butoxy)carbonylamino]-1-(cyanomethyl)pyrrole-2-carboxylate (6h)

From 1.07 g (4.9 mmol) **5h** was yielded 560 mg (40%) **6h** after flash chromatography in 7:2 hexanes/ethyl acetate as a white powder. TLC (8:5 hexanes/ethyl acetate) R_f 0.56 ^1H NMR(DMSO- d_6) δ 9.26 (s, 1H), 7.31 (s, 1H), 6.70 (s, 1H), 5.40 (s, 2H), 4.20 (q, 2H, $J=6.9$), 1.43 (s, 9H), 1.26 (t, 2H, $J=6.9$). E/I MS m/e 294.4 (M+H) (293.14 calcd. for $\text{C}_{14}\text{H}_{19}\text{N}_3\text{O}_4$).

4-[(tert-butoxy)carbonylamino]-1-(cyanomethyl)pyrrole-2-carboxylic acid (Boc-Py(CN)-OH) (7h)

From 340 mg (1.16 mmol) **6h** was yielded 300 mg (97%) **7h** as a white solid. TLC (1:1 hexanes/ethyl acetate) R_f 0.05 ^1H NMR(DMSO- d_6) δ 12.19 (bs, 1H), 9.09 (s, 1H), 7.09 (s, 1H), 6.57 (s, 1H), 4.92 (s, 2H), 1.42 (s, 9H). E/I MS m/e 264.0 (M-H) (265.11 calcd. for $\text{C}_{12}\text{H}_{15}\text{N}_3\text{O}_4$).

2,2,2-trichloro-1-[1-(2-methylpropyl)imidazol-2-yl]ethan-1-one (Im(iBu)-CK) (9)

(2-methylpropyl)imidazole (**8**) (10.0 g, 80.6 mmol) was mixed with 32 mL dichloromethane and added drop wise to a stirring solution of trichloroacetylchloride (14.74 g, 81.5 mmol) in 48 mL dichloromethane. The resulting solution was stirred at rt for 2 h. The reaction mixture was cooled to 0 °C and triethylamine (8.15 g, 80.6 mmol) was added drop wise. The triethylammonium chloride salt was filtered off and the mother liquor was concentrated *in vacuo*. The crude product was purified by flash chromatography in 2:1 hexanes/ethyl acetate to yield **9** (17.4 g, 84%) as a white powder. TLC (2:1 hexanes/ethyl acetate) R_f 0.46 ^1H NMR(DMSO- d_6) δ 7.77 (s, 1H), 7.36 (s, 1H),

4.23 (d, 2H, J=7.4), 1.95 (m, 1H), 0.83 (d, 6H, J=6.6). E/I MS m/e 269.1 (M+H) (267.99 calcd. for C₉H₁₁Cl₃N₂O).

2,2,2-trichloro 4-nitro-1-[1-(2-methylpropyl)imidazol-2-yl]ethan-1-one (10)

Compound **9** (1.0 g, 3.6 mmol) was dissolved in 10 mL acetic anhydride and cooled to an internal temperature of 0 °C. Fuming nitric acid (1.5 mL) was then added drop wise, followed by 0.5 mL concentrated H₂SO₄. The reaction mixture was slowly allowed to warm to room temperature where it was stirred overnight. After 10 h, the reaction was taken up in 25 mL water and the product extracted with ethyl acetate (2 x 50 mL). The combined organic layers were dried over sodium sulfate and concentrated *in vacuo*. The residue was then flash chromatographed in 4:1 hexanes/ethyl acetate to yield **10** (756 mg, 64%) as a pale yellow solid. TLC (3:1 hexanes/ethyl acetate) R_f 0.69 ¹H NMR(DMSO-*d*₆) δ 8.61 (s, 1H), 4.25 (d, 2H, J=7.2), 2.07 (m, 1H), 0.82 (d, 6H, J=6.6). E/I MS m/e 314.0 (M+H) (312.98 calcd. for C₉H₁₀Cl₃N₃O₃).

Ethyl 1-(2-methylpropyl)-4-nitroimidazole-2-carboxylate (11)

Compound **10** (450 mg, 1.38 mmol) was slurried with 5 mL ethanol and sodium hydride (60% dispersion in mineral oil, 100 mg) dissolved in 3 mL ethanol was added drop-wise over 10 min. The suspension was then heated to reflux for 30 min. The reaction was allowed to cool to rt and then was neutralized with cold 1 N HCl to pH7. The product was then extracted with chloroform (2 x 15 mL). Compound **11** (200 mg, 68%) was isolated without further purification as a clear oil. TLC (3:1 hexanes/ethyl acetate) R_f 0.31 ¹H NMR(DMSO-*d*₆) δ 8.56 (s, 1H), 4.25 (d, 2H, J=7.2), 3.41 (q, 2H, J=6.6), 2.08

(m, 1H), 1.03 (t, 2H, J=6.6), 0.83 (d, 6H, J=6.0). E/I MS m/e 242.1 (M+H) (241.11 calcd. for C₁₀H₁₅N₃O₄).

Polyamide Synthesis.

The parent polyamides ImPyPyPyPy-β-Dp (**PA1**) and ImImPyPyPy-β-Dp (**PA2**) were prepared according to standard solid-phase protocols.¹³

ImPyPy(Bz)PyPy-β-Dp (PA18) The manual solid-phase synthesis was performed as in previously published work.¹³ Boc-β-Ala-Pam-Resin (250 mg, 0.25 mmol) was swelled in DMF inside a 20 mL glass reaction vessel fitted with a glass filter and stopcock. The reaction vessel was drained after five minutes, the resin washed with 2 x 10 mL DCM, and deprotected with 50% TFA:DCM (10 mL). The vessel was shaken for 30 minutes and then drained and the resin washed with 3 x 10 mL DCM, 1 x 10 mL 4:1 DMF:DIEA, 1 x 10 mL DMF. Boc-Py-OBt (178 mg, 0.5 mmol) was added to the resin along with 1 mL NMP and 0.25 mL DIEA, and the reaction shaken at room temperature for two hours. A resin sample (4 mg) was taken out and cleaved in Dp at 90 °C for 10 minutes and used for HPLC analysis to verify completion of the coupling. 1 mL acetic anhydride was then added to the reaction and shaken for 10 minutes. The cycle was repeated for each new monomer using two equivalents of each Boc-protected monomer. Boc-Py(Bz)-OH, Boc-Ds-OH, Im-OH, and Boc-Im-OH were first activated with HBTU (1.0 equivalent) in NMP (1 mL) and DIEA (0.25 mL) for 5 minutes at room temperature. Im(iBu)-CCl₃ was added directly to the resin with 1 mL NMP and 0.25 mL DIEA and shaken at 37 °C for 2 h. When the polyamide synthesis was complete, the vessel was drained and washed with 2 x 10 mL each DMF, DCM, MeOH, and diethylether. Polyamide was cleaved from

resin in a glass vial with 2 mL Dp at 55 °C for 12 h. The cleavage product was purified by reversed phase HPLC. UV λ_{max} (H₂O) (ϵ) 312 nm (43,450). ¹H NMR (DMSO-*d*₆) δ 10.46 (s, 1H), 10.05 (s, 2H), 9.87 (s, 1H), 9.26 (bs, 1H), 8.02 (m, 2H), 7.38 (s, 1H), 7.34 (s, 1H), 7.27 (m, 3H), 7.18 (s, 1H), 7.16 (s, 1H), 7.13 (s, 2H), 7.10 (s, 2H), 7.03 (s, 1H), 6.85 (s, 1H), 5.59 (s, 2H), 3.97 (s, 3H), 3.82 (s, 3H), 3.81 (s, 3H), 3.77 (s, 3H), 3.35 (q, 2H, *J*=6.9), 3.08 (q, 2H, *J*=6.6), 2.98 (m, 2H), 2.72 (s, 3H), 2.71 (s, 3H), 2.32 (t, 2H, *J*=7.2), 1.71 (m, 2H). MALDI-TOF MS 846.34 (M+H) (845.42 calcd. for C₄₃H₅₁N₁₃O₆).

ImPyPyPyPy- β -Dp (PA1) UV λ_{max} (H₂O) (ϵ) 310 nm (43,450). ¹H NMR (DMSO-*d*₆) δ 10.47 (s, 1H), 9.56 (s, 1H), 9.93 (s, 1H), 9.89 (s, 1H), 9.20 (bs, 1H), 8.03 (m, 2H), 7.40 (s, 1H), 7.28 (s, 1H), 7.22 (m, 2H), 7.16 (s, 2H), 7.16 (s, 1H), 7.13 (s, 1H), 7.05 (s, 2H), 6.87 (s, 1H), 3.99 (s, 3H), 3.85 (s, 6H), 3.82 (s, 3H), 3.79 (s, 3H), 3.39 (q, 2H, *J*=6.0), 3.10 (q, 2H, *J*=6.0), 2.99 (m, 2H), 2.74 (s, 3H), 2.72 (s, 3H), 2.34 (t, 2H, *J*=7.2), 1.72 (m, 2H). MALDI-TOF MS 770.7 (M+H) (769.37 calcd. for C₃₆H₄₅N₁₃O₆).

ImImPyPyPy- β -Dp (PA2) UV λ_{max} (H₂O) (ϵ) 310 nm (43,450). ¹H NMR (DMSO-*d*₆) δ 10.35 (s, 1H), 9.96 (s, 1H), 9.89 (s, 1H), 9.76 (s, 1H), 9.20 (bs, 1H), 8.03 (m, 2H), 7.57 (s, 1H), 7.46 (s, 1H), 7.27 (d, 1H, *J*=1.8), 7.22 (d, 1H, *J*=1.7), 7.15 (s, 2H), 7.07 (s, 1H), 7.05 (d, 1H, *J*=1.8), 6.86 (d, 1H, *J*=1.7), 4.00 (s, 6H), 3.84 (s, 3H), 3.83 (s, 3H), 3.79 (s, 3H), 3.38 (q, 2H, *J*=6.0), 3.10 (q, 2H, *J*=5.7), 2.90 (m, 2H), 2.74 (s, 3H), 2.72 (s, 3H), 2.33 (t, 2H, *J*=7.8), 1.72 (m, 2H). MALDI-TOF MS 771.4 (M+H) (770.37 calcd. for C₃₆H₄₅N₁₃O₆).

ImPyPy(iBu)PyPy- β -Dp (PA3) UV λ_{max} (H2O) (ϵ) 311 nm (43,450). ^1H NMR (DMSO- d_6) δ 10.47 (s, 1H), 9.96 (s, 1H), 9.93 (s, 1H), 9.89 (s, 1H), 9.25 (bs, 1H), 8.03 (m, 2H), 7.39 (s, 1H), 7.28 (s, 1H), 7.24 (s, 1H), 7.19 (s, 1H), 7.15 (m, 3H), 7.04 (s, 2H), 6.86 (s, 1H), 4.11 (d, 2H, $J=6.0$), 3.98 (s, 3H), 3.84 (s, 3H), 3.82 (s, 3H), 3.78 (s, 3H), 3.36 (q, 2H, $J=6.6$), 3.09 (q, 2H, $J=6.0$), 2.98 (m, 2H), 2.73 (s, 3H), 2.71 (s, 3H), 2.33 (t, 2H, $J=6.6$), 1.97 (m, 1H), 1.71 (m, 2H), 0.79 (d, 6H, $J=6.6$). MALDI-TOF MS 812.5 (M+H) (811.43 calcd. for $\text{C}_{40}\text{H}_{53}\text{N}_{13}\text{O}_6$).

ImImPy(iBu)PyPy- β -Dp (PA4) UV λ_{max} (H2O) (ϵ) 311 nm (43,450). ^1H NMR (DMSO- d_6) δ 10.34 (s, 1H), 9.96 (s, 1H), 9.89 (s, 1H), 9.74 (s, 1H), 9.31 (bs, 1H), 8.04 (m, 2H), 7.56 (s, 1H), 7.45 (s, 1H), 7.30 (s, 1H), 7.20 (s, 1H), 7.15 (s, 1H), 7.10 (s, 1H), 7.07 (s, 1H), 7.03 (s, 1H), 6.86 (s, 1H), 4.11 (d, 2H, $J=6.6$), 3.99 (s, 6H), 3.82 (s, 3H), 3.80 (s, 3H), 3.36 (q, 2H, $J=6.6$), 3.09 (q, 2H, $J=6.6$), 2.97 (m, 2H), 2.72 (s, 3H), 2.71 (s, 3H), 2.32 (t, 2H, $J=6.6$), 1.96 (m, 1H), 1.72 (m, 2H), 0.78 (d, 6H, $J=5.6$). MALDI-TOF MS 813.45 (M+H) (812.43 calcd. for $\text{C}_{39}\text{H}_{52}\text{N}_{14}\text{O}_6$).

ImImPyPy(iBu)Py- β -Dp (PA5) UV λ_{max} (H2O) (ϵ) 311 nm (43,450). ^1H NMR (DMSO- d_6) δ 10.34 (s, 1H), 9.96 (s, 1H), 9.88 (s, 1H), 9.75 (s, 1H), 9.30 (bs, 1H), 8.04 (m, 2H), 7.56 (s, 1H), 7.45 (s, 1H), 7.27 (s, 1H), 7.23 (s, 1H), 7.15 (s, 1H), 7.14 (s, 1H), 7.07 (s, 1H), 7.02 (s, 1H), 6.84 (s, 1H), 4.10 (d, 2H, $J=7.2$), 3.99 (s, 6H), 3.84 (s, 3H), 3.78 (s, 3H), 3.35 (q, 2H, $J=6.0$), 3.09 (q, 2H, $J=6.3$), 2.98 (m, 2H), 2.72 (s, 3H), 2.71 (s, 3H), 2.33 (t, 2H, $J=7.2$), 1.96 (m, 1H), 1.71 (m, 2H), 0.78 (d, 6H, $J=6.3$). MALDI-TOF MS 813.45 (M+H) (812.43 calcd. for $\text{C}_{39}\text{H}_{52}\text{N}_{14}\text{O}_6$).

ImPy(Am)PyPyPy- β -Dp (PA6) This polyamide was made by two distinct methods. In the first method, Each monomeric unit was coupled using the standard solid phase methodology. The Py(Am) unit was incorporated as the Boc-Py(CN)-OH (**7h**) which was hydrated by trace amounts of water in the subsequent acidic deprotection steps. Alternatively, **PA10** (10 μ Mol) was dissolved in 0.5 mL anhydrous DMF. NaH (80 μ Mol) was then added and the reaction allowed to sit at 0 °C for 15 minutes. Bromoacetamide (10 μ Mol) was then added and the reaction monitored by rp-HPLC. After 10 minutes, the reaction was complete and was quenched by the addition of 7.5 mL 0.1% TFA and purified by reversed-phase HPLC (50% yield). UV λ_{max} (H2O) (ϵ) 311 nm (43,450). ^1H NMR (DMSO- d_6) δ 10.49 (s, 1H), 9.97 (s, 1H), 9.94 (s, 1H), 9.88 (s, 1H), 9.28 (bs, 1H), 8.03 (m, 2H), 7.40 (s, 1H), 7.29 (s, 1H), 7.28 (s, 1H), 7.21 (m, 3H), 7.15 (d, 1H, $J=1.8$), 7.06 (s, 2H), 7.03 (d, 1H, $J=2.1$), 7.01 (d, 1H, $J=1.5$), 6.86 (d, 1H, $J=1.5$), 4.95 (s, 2H), 3.99 (s, 3H), 3.84 (s, 3H), 3.83 (s, 3H), 3.79 (s, 3H), 3.37 (q, 2H, $J=6.0$), 3.10 (q, 2H, $J=6.0$), 2.98 (m, 2H), 2.74 (s, 3H), 2.72 (s, 3H), 2.34 (t, 2H, $J=7.2$), 1.73 (m, 2H). MALDI-TOF MS 813.6 (M+H) (812.39 calcd. for $\text{C}_{38}\text{H}_{48}\text{N}_{14}\text{O}_7$).

ImImPyPy(Am)Py- β -Dp (PA7) See **PA6** for synthesis. UV λ_{max} (H2O) (ϵ) 311 nm (43,450). ^1H NMR (DMSO- d_6) δ 10.35 (s, 1H), 9.99 (s, 1H), 9.91 (s, 1H), 9.73 (s, 1H), 9.30 (bs, 1H), 8.03 (m, 2H), 7.56 (s, 1H), 7.45 (s, 1H), 7.24 (s, 1H), 7.22 (s, 1H), 7.21 (s, 1H), 7.15 (s, 1H), 7.12 (s, 1H), 7.09 (s, 1H), 7.07 (s, 1H), 6.99 (m, 1H), 6.83 (s, 1H), 4.93 (s, 2H), 3.99 (s, 6H), 3.84 (s, 3H), 3.78 (s, 3H), 3.36 (q, 2H, $J=6.6$), 3.09 (q, 2H, $J=6.0$), 2.98 (m, 2H), 2.73 (s, 3H), 2.71 (s, 3H), 2.33 (t, 2H, $J=6.6$), 1.73 (m, 2H). MALDI-TOF MS 814.5 (M+H) (813.41 calcd. for $\text{C}_{37}\text{H}_{47}\text{N}_{15}\text{O}_7$).

ImPyDsPyPy- β -Dp (PA8) UV λ_{max} (H₂O) (ϵ) 316 nm (43,450). ¹H NMR (DMSO-*d*₆) δ 11.21 (s, 1H), 10.48 (s, 1H), 9.95 (s, 1H), 9.93 (s, 1H), 9.91 (s, 1H), 9.34 (bs, 1H), 8.04 (m, 2H), 7.41 (s, 1H), 7.29 (d, 1H, *J*=2.1), 7.24 (d, 1H, *J*=1.8), 7.16 (m, 4H), 7.07 (d, 1H, *J*=3.0), 7.00 (d, 1H, *J*=1.8), 6.86 (d, 1H, *J*=1.8), 3.99 (s, 3H), 3.85 (s, 3H), 3.84 (s, 3H), 3.80 (s, 3H), 3.37 (q, 2H, *J*=5.7), 3.10 (q, 2H, *J*=6.3), 3.00 (m, 2H), 2.74 (s, 3H), 2.72 (s, 3H), 2.34 (t, 2H, *J*=7.8), 1.74 (m, 2H). MALDI-TOF MS 756.5 (M+H) (755.37 calcd. for C₃₆H₄₅N₁₃O₆).

ImImDsPyPy- β -Dp (PA9) UV λ_{max} (H₂O) (ϵ) 316 nm (43,450).

ImDsPyPyPy- β -Dp (PA10) UV λ_{max} (H₂O) (ϵ) 316 nm (43,450). ¹H NMR (DMSO-*d*₆) δ 11.30 (s, 1H), 10.46 (s, 1H), 9.95 (s, 2H), 9.89 (s, 1H), 9.27 (bs, 1H), 8.03 (m, 2H), 7.40 (s, 1H), 7.27 (d, 1H, *J*=2.1), 7.24 (d, 1H, *J*=1.8), 7.21 (m, 2H), 7.15 (d, 1H, *J*=1.8), 7.06 (s, 2H), 7.02 (d, 1H, *J*=1.8), 6.87 (d, 1H, *J*=1.8), 3.99 (s, 3H), 3.85 (s, 3H), 3.83 (s, 3H), 3.79 (s, 3H), 3.36 (q, 2H, *J*=6.0), 3.10 (q, 2H, *J*=6.3), 2.95 (m, 2H), 2.74 (s, 3H), 2.72 (s, 3H), 2.34 (t, 2H, *J*=7.2), 1.73 (m, 2H). MALDI-TOF MS 756.5 (M+H) (755.37 calcd. for C₃₆H₄₅N₁₃O₆).

ImImPyDsPy- β -Dp (PA11) UV λ_{max} (H₂O) (ϵ) 316 nm (43,450). ¹H NMR (DMSO-*d*₆) δ 11.18 (s, 1H), 10.34 (s, 1H), 9.95 (s, 1H), 9.89 (s, 1H), 9.731 (s, 1H), 9.24 (bs, 1H), 8.04 (m, 2H), 7.57 (s, 1H), 7.46 (s, 1H), 7.27 (s, 1H), 7.18 (s, 1H), 7.14 (m, 3H), 7.07 (s, 1H), 6.80 (d, 1H, *J*=1.8), 3.99 (s, 6H), 3.84 (s, 3H), 3.79 (s, 3H), 3.37 (q, 2H, *J*=5.7), 3.10

(q, 2H, J=6.3), 3.00 (m, 2H), 2.74 (s, 3H), 2.72 (s, 3H), 2.34 (t, 2H, J=7.8), 1.72 (m, 2H).

MALDI-TOF MS 757.4 (M+H) (756.37 calcd. for C₃₆H₄₅N₁₃O₆).

ImPyPy(2Am)PyPy-β-Dp (P12) UV λ_{max} (H₂O) (ε) 311 nm (43,450). MALDI-TOF MS 827.6 (M+H) (826.41 calcd. for C₃₉H₅₁N₁₄O₆).

ImPyPy(2P)PyPy-β-Dp (PA13) UV λ_{max} (H₂O) (ε) 311 nm (43,450). ¹H NMR (DMSO-d₆) δ 10.49 (s, 1H), 10.14 (s, 1H), 9.90 (s, 1H), 9.71 (s, 1H), 9.40 (bs, 1H), 8.04 (m, 2H), 7.93 (bs, 3H), 7.58 (d, 1H, J=5.7), 7.45 (s, 2H), 7.26 (s, 1H), 7.25 (s, 1H), 7.15 (s, 1H), 7.06 (d, 1H, J=2.7), 6.98 (s, 1H), 6.85 (s, 1H), 4.44 (t, 2H, J=6.0), 3.99 (s, 6H), 3.83 (s, 3H), 3.78 (s, 3H), 3.35 (q, 2H, J=5.4), 3.22 (m, 2H), 3.09 (q, 2H, J=6.0), 2.98 (m, 2H), 2.72 (s, 3H), 2.71 (s, 3H), 2.32 (t, 2H, J=5.4), 1.72 (m, 2H). MALDI-TOF MS 800.71 (M+H) (799.41 calcd. for C₃₇H₄₉N₁₅O₆).

ImPyPy(3P)PyPy-β-Dp (PA14) UV λ_{max} (H₂O) (ε) 311 nm (43,450). ¹H NMR (DMSO-d₆) δ 10.48 (s, 1H), 10.04 (s, 2H), 9.90 (s, 1H), 9.30 (bs, 1H), 8.05 (m, 2H), 7.71 (bs, 3H), 7.40 (s, 2H), 7.29 (s, 1H), 7.26 (s, 1H), 7.18 (d, 1H, J=1.5), 7.15 (d, 1H, J=1.5), 7.09 (s, 1H), 7.05 (s, 1H), 6.99 (s, 1H), 6.87 (s, 1H), 4.37 (t, 2H, J=5.4), 3.98 (s, 3H), 3.84 (s, 3H), 3.83 (s, 3H), 3.79 (s, 3H), 3.36 (q, 2H, J=5.9), 3.10 (q, 2H, J=6.0), 3.00 (m, 2H), 2.77 (t, 2H, J=4.2), 2.74 (s, 3H), 2.72 (s, 3H), 2.34 (t, 2H, J=6.6), 1.99 (m, 2H), 1.72 (m, 2H). MALDI-TOF MS 813.5 (M+H) (812.41 calcd. for C₃₉H₅₂N₁₄O₆).

ImImPy(3P)PyPy-β-Dp (PA15) UV λ_{max} (H2O) (ϵ) 311 nm (43,450). MALDI-TOF MS 814.45 (M+H) (813.41 calcd. for $\text{C}_{38}\text{H}_{51}\text{N}_{15}\text{O}_6$).

ImPyPy(3G)PyPy-β-Dp (PA16) **PA14** (1.6 μmol) was dissolved in 0.12 mL CH_3CN . 0.06 mL of a 0.387 M (16 μmol) solution of N,N'-Boc-guanidyl pyrazole was added and the reaction heated to 75 °C for 2 h. The solvent was removed *in vacuo* and the residue taken up in 0.2 mL 50% TFA:DCM. After 2 h at room temperature, the solvent was evaporated and the residue taken up in 0.1% TFA. **PA16** was purified by reversed phase HPLC. UV λ_{max} (H2O) (ϵ) 311 nm (43,450). ^1H NMR (DMSO-d_6) δ 10.49 (s, 1H), 9.98 (s, 2H), 9.93 (s, 1H), 9.34 (bs, 1H), 8.05 (m, 2H), 7.41 (s, 1H), 7.30 (s, 1H), 7.297 (s, 1H), 7.28 (s, 1H), 7.26 (m, 2H), 7.24 (s, 1H), 7.21 (s, 1H), 7.18 (t, 2H, $J=1.5$), 7.11 (d, 1H, $J=1.5$), 7.08 (d, 1H, $J=1.5$), 7.07 (d, 1H, $J=1.5$), 4.51 (t, 2H, $J=6.0$), 4.00 (s, 3H), 3.86 (s, 3H), 3.85 (s, 3H), 3.81 (s, 3H), 3.37 (m, 4H), 3.11 (q, 2H, $J=6.0$), 3.00 (m, 4H), 2.75 (s, 3H), 2.73 (s, 3H), 2.35 (t, 2H, $J=7.2$), 1.73 (m, 2H) MALDI-TOF MS 855.66 (M+H) (854.45 calcd. for $\text{C}_{40}\text{H}_{54}\text{N}_{16}\text{O}_6$).

ImPyPy(5F)PyPy-β-Dp (PA17) UV λ_{max} (H2O) (ϵ) 314 nm (43,450). ^1H NMR (DMSO-d_6) δ 10.47 (s, 1H), 10.05 (s, 1H), 9.98 (s, 1H), 9.91 (s, 1H), 9.46 (bs, 1H), 8.04 (m, 2H), 7.39 (s, 1H), 7.26 (s, 1H), 7.23 (d, 1H, $J=1.8$), 7.17 (s, 1H), 7.15 (s, 2H), 7.04 (s, 1H), 7.03 (d, 1H, $J=1.8$), 7.01 (d, 1H, $J=1.9$), 6.87 (d, 1H, $J=1.8$), 5.66 (s, 2H), 3.97 (s, 3H), 3.83 (s, 3H), 3.81 (s, 3H), 3.78 (s, 3H), 3.33 (q, 2H, $J=5.4$), 3.09 (q, 2H, $J=6.0$), 2.97 (m, 2H), 2.72 (s, 3H), 2.71 (s, 3H), 2.33 (t, 2H, $J=6.6$), 1.72 (m, 2H). MALDI-TOF MS 936.4 (M+H) (935.37 calcd. for $\text{C}_{43}\text{H}_{47}\text{F}_5\text{N}_{13}\text{O}_6$).

ImImPy(Bz)PyPy- β -Dp (PA19) UV λ_{max} (H2O) (ϵ) 312 nm (43,450). ^1H NMR (DMSO- d_6) δ 10.41 (s, 1H), 10.03 (s, 1H), 9.87 (s, 1H), 9.72 (s, 1H), 9.29 (bs, 1H), 8.02 (m, 2H), 7.56 (d, 1H, $J=2.4$), 7.44 (d, 1H, $J=1.5$), 7.42 (s, 1H), 7.28 (m, 1H), 7.26 (d, 1H, $J=1.5$), 7.19 (m, 1H), 7.16 (s, 1H), 7.14 (s, 1H), 7.13 (s, 1H), 7.12 (s, 1H), 7.10 (s, 1H), 7.06 (d, 1H, $J=2.7$), 7.02 (s, 1H), 6.85 (s, 1H), 5.59 (s, 2H), 3.98 (s, 6H), 3.80 (s, 3H), 3.77 (s, 3H), 3.35 (q, 2H, $J=6.0$), 3.08 (q, 2H, $J=6.0$), 2.98 (m, 2H), 2.72 (s, 3H), 2.70 (s, 3H), 2.32 (t, 2H, $J=6.6$), 1.71 (m, 2H). MALDI-TOF MS 847.28 (M+H) (846.41 calcd. for $\text{C}_{42}\text{H}_{51}\text{N}_{14}\text{O}_6$).

ImPyPy(2Bz)PyPy- β -Dp (PA20) UV λ_{max} (H2O) (ϵ) 312 nm (43,450).

ImImPy(2Bz)PyPy- β -Dp (PA21) UV λ_{max} (H2O) (ϵ) 312 nm (43,450). ^1H NMR (DMSO- d_6) δ 10.33 (s, 1H), 9.99 (s, 1H), 9.90 (s, 1H), 9.73 (s, 1H), 9.36 (bs, 1H), 8.03 (m, 2H), 7.56 (s, 1H), 7.45 (s, 1H), 7.28 (s, 2H), 7.24 (s, 1H), 7.23 (s, 2H), 7.21 (m, 1H), 7.19 (s, 1H), 7.15 (m, 2H), 7.06 (m, 2H), 6.86 (s, 1H), 4.49 (t, 2H, $J=6.0$), 3.99 (s, 6H), 3.84 (s, 3H), 3.78 (s, 3H), 3.36 (q, 2H, $J=6.0$), 3.09 (q, 2H, $J=6.0$), 2.98 (m, 4H), 2.72 (s, 3H), 2.71 (s, 3H), 2.33 (t, 2H, $J=6.6$), 1.72 (m, 2H). MALDI-TOF MS 861.16 (M+H) (860.43 calcd. for $\text{C}_{43}\text{H}_{52}\text{N}_{14}\text{O}_6$).

ImPyPy(In)PyPy- β -Dp (PA22) UV λ_{max} (H2O) (ϵ) 314 nm (43,450). ^1H NMR (DMSO- d_6) δ 10.47 (s, 1H), 9.86 (s, 2H), 9.73 (s, 1H), 9.19 (bs, 1H), 8.03 (m, 2H), 7.39 (s, 1H), 7.31 (s, 1H), 7.21 (s, 1H), 7.19 (s, 1H), 7.16 (s, 1H), 7.14 (s, 1H), 7.04 (s, 1H), 7.02 (s, 1H), 6.94 (m, 1H), 6.85 (s, 1H), 6.60 (m, 1H), 6.55 (m, 1H), 5.32 (d, 1H), 4.54 (s,

2H), 4.48 (bs, 1H), 3.98 (s, 3H), 3.87 (s, 3H), 3.81 (s, 3H), 3.78 (s, 3H), 3.09 (q, 2H, J=6.3), 2.98 (m, 2H), 2.72 (s, 3H), 2.71 (s, 3H), 2.32 (t, 2H, J=6.6), 1.71 (m, 2H)
MALDI-TOF MS 887.51 (M+H) (886.44 calcd. for C₄₅H₅₄N₁₄O₆).

Im(iBu)DsPyPyPy(iBu)-β-Dp (PA23) UV λ_{max} (H₂O) (ε) 316 nm (43,450). ¹H NMR (DMSO-d₆) δ 11.23 (s, 1H), 10.44 (s, 1H), 9.96 (s, 2H), 9.90 (s, 1H), 9.20 (bs, 1H), 8.03 (m, 2H), 7.41 (s, 1H), 7.30 (s, 1H), 7.24 (s, 1H), 7.22 (s, 1H), 7.18 (s, 1H), 7.17 (s, 1H), 7.06 (s, 1H), 7.05 (d, 1H, J=1.8), 7.01 (s, 1H), 6.85 (s, 1H), 4.28 (d, 2H, J=7.8), 4.06 (d, 2H, J=6.6), 3.84 (s, 3H), 3.83 (s, 3H), 3.08 (m, 2H), 2.97 (m, 2H), 2.74 (s, 3H), 2.72 (s, 3H), 2.34 (t, 2H, J=7.2), 2.07 (m, 1H), 1.92 (m, 1H), 1.76 (m, 2H), 0.83 (d, 6H, J=6.3), 0.77 (d, 6H, J=6.3) MALDI-TOF MS 840.8 (M+H) (839.46 calcd. for C₄₂H₅₇N₁₃O₆).

ImImPy(iBu)DsPy-β-Dp (PA24) UV λ_{max} (H₂O) (ε) 316 nm (43,450). ¹H NMR (DMSO-d₆) δ 11.20 (s, 1H), 10.36 (s, 1H), 9.96 (s, 1H), 9.91 (s, 1H), 9.74 (s, 1H), 9.30 (bs, 1H), 8.07 (m, 2H), 7.58 (s, 1H), 7.47 (s, 1H), 7.32 (d, 1H, J=1.8), 7.20 (d, 1H, J=1.5), 7.17 (s, 1H), 7.12 (s, 2H), 7.08 (s, 1H), 6.82 (d, 1H, J=1.8), 4.13 (d, 2H, J=6.9), 4.02 (s, 3H), 4.01 (s, 3H), 3.81 (s, 3H), 3.39 (q, 2H, J=6.6), 3.11 (q, 2H, J=5.7), 3.00 (m, 2H), 2.75 (s, 3H), 2.73 (s, 3H), 2.35 (t, 2H, J=7.2), 1.99 (m, 1H), 1.74 (m, 2H), 0.81, (d, 6H, J=6.6). MALDI-TOF MS 799.5 (M+H) (798.41 calcd. for C₃₈H₅₀N₁₄O₆).

Preparation of 3' ³²P-end Labeled Restriction Fragments.

Plasmid pDHN2 was cut using *PvuII* and *EcoRI* to yield a 250 bp restriction fragment containing the binding sites 5'-caTGGTACAt-3', 5'-caTGGTCCAt-3', and 5'-

caTGTTACAt-3'. The sticky ends of the fragment were filled in using Sequenase, [α - 32 P]-deoxyadenosine-5'-triphosphate, and [α - 32 P]-thymidine-5'-triphosphate. The labeled fragment was then purified by nondenaturing gel electrophoresis. A and G sequencing were performed as previously described.¹⁷

Quantitative DNase I Footprinting Titrations.

Polyamide/DNA equilibrations and DNase I footprinting were performed, and equilibrium association constants determined, as previously described for all homodimer experiments. In heterodimer experiments, the polyamide concentration reported is the concentration of each individual polyamide. Thus, a 100 nM equilibration will contain each of the two polyamides at 100 nM for a total polyamide concentration of 200 nM. All other experimental parameters remain unchanged from the homodimer protocol.⁹

References.

1. Stryer, L., *Biochemistry*. W. H. Freeman and Co.: New York, 1995.
2. Ban, N.; Nissen, P.; Hansen, J.; Moore, P. B.; Steitz, T. A., *Science*, **2000**, 289, 905–920.
3. Gallivan, J. P.; Dougherty, D. A., *Proceedings of the National Academy of Sciences of the United States of America*, **1999**, 96, 9459–9464.
4. Gallivan, J. P.; Dougherty, D. A., *Journal of the American Chemical Society*, **2000**, 122, 870–874.
5. Ma, J. C.; Dougherty, D. A., *Chemical Reviews*, **1997**, 97, 1303–1324.
6. West, A. P.; Mecozzi, S.; Dougherty, D. A., *Journal of Physical Organic Chemistry*, **1997**, 10, 347–350.
7. Kielkopf, C. L.; Baird, E. E.; Dervan, P. B.; Rees, D. C., *Nature Struct. Biol.*, **1998**, 5, 104.
8. Trauger, J. W., *Ph. D. Thesis*, California Institute of Technology, Pasadena, **1998**, 77.
9. Trauger, J. W.; Dervan, P. B., Footprinting methods for analysis of pyrrole-imidazole polyamide/DNA complexes. In *Drug-Nucleic Acid Interactions*, 2001; Vol. 340, pp 450–466.
10. Pardo, C.; et al., *OPPI Briefs*, **2000**, 4, 385–390.
11. Rucker, V. C.; Fostier, S.; Melander, C.; Dervan, P. B., *Journal of the American Chemical Society*, **2003**, 125, 1195–1202.
12. Bremer, R. E.; Szewczyk, J. W.; Baird, E. E.; Dervan, P. B., *Bioorganic & Medicinal Chemistry*, **2000**, 8, 1947–1955.
13. Baird, E. E.; Dervan, P. B., *Journal of the American Chemical Society*, **1996**, 118, 6141–6146.
14. Nguyen, D. H., *Ph. D. Thesis*, **2001**.
15. Doherty, E. A.; Doudna, J. A., *Annual Review of Biochemistry*, **2000**, 69, 597–615.
16. Pandolfi, P. P., *Oncogene*, **2001**, 20, 3116–3127.
17. Maxam, A. M.; Gilbert, W. S., *Methods in Enzymology*, **1980**, 65, 499.